

BULLETIN N° 227
ACADÉMIE EUROPÉENNE
INTERDISCIPLINAIRE
DES SCIENCES
INTERDISCIPLINARY EUROPEAN ACADEMY OF SCIENCES



Lundi 10 septembre 2018 16h à l'Institut Henri Poincaré salle 01:

Conférence

" *Electronique quantique dans les nanoconducteurs* "

par le Pr Gwendal FÈVE

Université Paris VI Sorbonne, Laboratoire de Physique

Pierre AIGRAIN de l'ENS Ulm

Notre Prochaine séance aura lieu le lundi 1er octobre 2018

à 16h

à l'Institut Henri Poincaré salle 01

11, rue Pierre et Marie Curie 75005 PARIS/Métro : RER Luxembourg

Elle aura pour thème

Conférence

" *Transport électronique quantique* "

par Gilles MONTAMBAUX

Directeur de Recherche de classe exceptionnelle CNRS

Laboratoire de Physique des Solides, Orsay

Professeur à l'École Polytechnique

ACADÉMIE EUROPÉENNE INTERDISCIPLINAIRE DES SCIENCES INTERDISCIPLINARY EUROPEAN ACADEMY OF SCIENCES

PRÉSIDENT : Pr Victor MASTRANGELO
VICE PRÉSIDENT : Pr Jean-Pierre FRANÇOISE
VICE PRÉSIDENT BELGIQUE(Liège):
 Pr Jean SCHMETS
VICE PRÉSIDENT ITALIE(Rome):
 Pr Ernesto DI MAURO
SECRÉTAIRE GÉNÉRALE : Irène HERPE-LITWIN
TRÉSORIÈRE GÉNÉRALE: Édith PERRIER

MEMBRES CONSULTATIFS DU CA :
 Gilbert BELAUBRE
 François BÉGON
 Bruno BLONDEL
 Michel GONDRAN

COMMISSION FINANCES: Claude ELBAZ
COMMISSION MULTIMÉDIA: Pr. Alain CORDIER
COMMISSION SYNTHÈSES SCIENTIFIQUES:
 Jean-Pierre TREUIL
COMMISSION CANDIDATURES:
 Pr. Jean-Pierre FRANÇOISE

PRÉSIDENT FONDATEUR : Dr. Lucien LÉVY (†)
PRÉSIDENT D'HONNEUR : Gilbert BELAUBRE

CONSEILLERS SCIENTIFIQUES :
SCIENCES DE LA MATIÈRE : Pr. Gilles COHEN-TANNOUJJI
SCIENCES DE LA VIE ET BIOTECHNIQUES : Pr Ernesto DI MAURO

CONSEILLERS SPÉCIAUX:
ÉDITION: Pr Robert FRANCK
AFFAIRES EUROPÉENNES :Pr Jean SCHMETS
RELATIONS VILLE DE PARIS et IDF:
 Michel GONDRAN ex-Président/ Claude MAURY
MOYENS MULTIMÉDIA et RELATIONS UNIVERSITÉS:
 Pr Alain CORDIER
RELATIONS AX: Gilbert BELAUBRE
MECENAT: Pr Jean Félix DURASTANTI
**GRANDS ORGANISMES DE RECHERCHE NATIONAUX ET
INTERNATIONAUX**: Pr Michel SPIRO

SECTION DE NANCY :
PRESIDENT : Pr Pierre NABET

septembre 2018

N°227

TABLE DES MATIERES

p. 03 Séance du 10 septembre 2018:
 p. 05 Annonces
 p. 07 Documents

Prochaine séance : lundi 1er octobre 2018 IHP à 16h salle 01

Conférence
"Transport électronique quantique "
par Gilles MONTAMBAUX
Directeur de Recherche de classe exceptionnelle CNRS
Laboratoire de Physique des Solides, Orsay
Professeur à l'École Polytechnique

**ACADEMIE EUROPEENNE INTERDISCIPLINAIRE DES SCIENCES
INTERDISCIPLINARY EUROPEAN ACADEMY OF SCIENCES**

5 rue Descartes 75005 PARIS

Séance du Lundi 10 septembre 2018/Institut Henri Poincaré salle 01

La séance est ouverte à 16h, **sous la Présidence de Victor MASTRANGELO** et en la présence de nos Collègues Gilbert BELAUBRE, Jean-Louis BOBIN, Gilles COHEN-TANNOUDJI, Sylvie DERENNE, Jean Félix DURASTANTI, Françoise DUTHEIL, Claude ELBAZ, Michel GONDRAN, Irène HERPELITWIN, Claude MAURY, Edith PERRIER, Jacques PRINTZ, Jean SCHMETS..

Sont excusés: François BEGON, Jean-Pierre BESSIS, Bruno BLONDEL, Michel CABANAC, Alain CARDON, Alain CORDIER, Juan-Carlos CHACHQUES, Eric CHENIN, Ernesto DI MAURO, Vincent FLEURY, Jean-Pierre FRANÇOISE, Dominique LAMBERT, Gérard LEVY, Antoine LONG, Pierre MARCHAIS, Anastassios METAXAS, Jean-Jacques NIO, Alberto OLIVIERO, Marie-Françoise PASSINI, Michel SPIRO, Alain STAHL, Jean-Paul TEYSSANDIER, Jean VERDETTI

Etaient présents en tant que visiteurs de jeunes chercheurs du Laboratoire Pierre AIGRAIN de l'ENS à savoir Hugo BARTOLOMEI, Erwann BOCQUILLON, Holger GRAEF, David MELE

I. Présentation du conférencier par notre Président Victor MASTRANGELO

Gwendal FEVE fait sa thèse au Laboratoire Pierre Aigrain du département de Physique de l'Ecole Normale Supérieure sous la direction de Bernard PLAÇAIS et Christian GLATTLI (thèse soutenue en 2006). Sa thèse portait sur la réalisation d'une source d'électron permettant de générer un électron à la demande dans un conducteur électrique et d'étudier ainsi les courants électriques à l'échelle élémentaire de l'électron unique.

Il a ensuite fait un séjour postdoctoral d'une année au Laboratoire de Photonique et Nanostructures (LPN) à Marcoussis.

Il a ensuite été recruté comme Maître de Conférences au département de Physique de l'ENS puis en 2013 comme Professeur à Sorbonne Université (anciennement Université Pierre et Marie Curie).

Il est membre junior de l'Institut Universitaire de France depuis 2014. Il effectue sa recherche au sein du groupe de Physique Mésoscopique (dirigé par Bernard PLAÇAIS) du Laboratoire Pierre Aigrain au département de Physique de l'ENS. Au sein de ce groupe il conduit les recherches portant sur l'étude des courants électriques quantiques qui sont constitués de un à quelques électrons. Ces recherches visent à établir les signatures de la Physique quantique sur la propagation des courants électriques

II. Conférence du Pr Gwendal FEVE : " *Electronique quantique dans les nanoconducteurs* "

Résumé de la conférence avec références bibliographiques:

"Electronique quantique dans les nanoconducteurs"

Les progrès des techniques de nanofabrication de l'industrie du semi-conducteur permettent maintenant de façonner les conducteurs électriques à l'échelle de la dizaine de nanomètres. A cette échelle, la matière acquiert de nouvelles propriétés gouvernées par la physique quantique. Le transport des électrons dans un tel

conducteur (en particulier à basse température) n'est plus décrit par le mouvement de corpuscules classiques mais par la propagation d'ondes de matière analogues aux ondes lumineuses de l'optique. Je présenterai dans cet exposé des expériences illustrant cette optique électronique dans les conducteurs quantiques.

References:

Electron quantum optics in ballistic chiral conductors

Erwann Bocquillon, Vincent Freulon, François D Parmentier, Jean-Marc Berroir, Bernard Plaçais, Claire Wahl, Jérôme Rech, Thibaut Jonckheere, Thierry Martin, Charles Grenier, Dario Ferraro, Pascal Degiovanni, Gwendal Fève, *Annalen der Physik*, 526 1 (2014).

Coherence and indistinguishability of single electrons emitted by independent sources

Erwann Bocquillon, Vincent Freulon, J-M Berroir, Pascal Degiovanni, Bernard Plaçais, A Cavanna, Yong Jin, Gwendal Fève, *Science* 339, 1054 (2013).

Un compte-rendu détaillé, voire un enregistrement audio-vidéo sera prochainement disponible sur le site de l'AEIS , <http://www.science-inter.com>

Annonces

- I. Notre président vous informe de la parution de l'ouvrage relatif à notre colloque de 2016 " ONDES , MATIÈRE ET UNIVERS" chez EDP sciences. **La version PDF est d'ores et déjà disponible en Open-Access sur le site d'EDP-Sciences :**
https://www.edp-open.org/books-in-french#Ondes_matiere_et_Univers

La version papier est également disponible:

Coût de l'ouvrage papier : 40€

Mode d'acquisition : adresser à notre Trésorière Edith PERRIER un chèque ou un virement correspondant aux nombres d'exemplaires souhaités.

Coordonnées Edith PERRIER:

PERRIER Edith	Bonneval 19120 PUY D'ARNAC	edith.perrier@ird.fr	01 48 02 59 69	06 83 05 72 04
---------------	----------------------------	--	----------------	----------------

(Si nécessaire elle vous communiquera le RIB de virement)

Dès que notre Trésorière aura perçu les fonds, les ouvrages vous seront remis lors de la prochaine séance de l'AEIS.

- II. Notre Collègue de Nancy, Jean Louis REYNET vient de publier auprès des Editions *Sydney Laurent*, un nouvel ouvrage intitulé : "**Les interactions dans l'art du paléolithique supérieur** ". Voici le résumé:

L'art paléolithique est généralement considéré comme dénué d'action : ce n'est que plus tard au Néolithique que les scènes interactives (chasses, guerres ou autres) d'un seul coup foisonnent. De ce fait, les scènes interactives au Paléolithique (une centaine au total) ont rarement fait l'objet d'études d'ensemble. L'ouvrage les recense, les catégorise, propose une méthodologie d'analyse et en donne une lecture individualisée. Enfin, il livre quelques conclusions et tente de resituer les résultats au regard des principales théories explicatives de l'art au Paléolithique.

- III. Notre Collègue Jacques PRINTZ , nous fait part de la parution auprès de l'éditeur *Les acteurs du savoir* de son dernier ouvrage "**Survivrons nous à la technologie? aux sources du cyberspace et des sciences de la complexité**". En voici la présentation:

Le cyberspace qui se construit sous nos yeux n'aurait pas pu exister sans l'invention d'une machine qui n'aurait jamais dû fonctionner tant les obstacles pour la construire étaient nombreux: l'ordinateur, le computing instrument de von Neumann, que chacun manipule quotidiennement, le smartphone de la « Petite Poucette » de Michel Serres.
 Pour savoir où l'on va, mieux vaut savoir d'où l'on vient! Pour résoudre les problèmes auxquels les démocraties furent confrontées lors de la Seconde guerre Mondiale: il fallait calculer, vite, communiquer, vite, sans erreur, comprendre les pannes; il fallait intégrer les technologies et coordonner les efforts de milliers d'ingénieurs qui ont conçu et exploité les systèmes sans lesquels nous n'aurions pas survécu aux totalitarismes. autant de problèmes d'éthique auxquels il est urgent de réfléchir.

Von Neumann, peu de temps avant sa mort, en 1955, nous a donné une clé, dans son article au magazine Fortune, et intitulé Survivrons-nous à la technologie?: « Nous pouvons spécifier seulement les qualités humaines nécessaires: patience, flexibilité, intelligence ». tel est le sujet des six chapitres de cet ouvrage.

L'ouvrage de (22€franco de port)) peut être commandé sur le site www.saintlegerproductions.fr ou en remplissant le bon de commande ci-dessous :

je commande..... exemplaire(s) du livre Survivrons-nous à la technologie
 au prix unitaire de 22 euros (franco de port)
Total =..... euros (franco de port)
que je règle par chèque bancaire joint à ce courrier et libellé à l'ordre de
Saint-Léger productions, 1, chemin des pièces Bron 49260 Le Coudray-Macouard
 ou par virement bancaire IBAN FR76 1027 8394 3700 0217 0820 246

Nom – Prénom.....
 Société.....
 Adresse.....

 Code postal.....
 Ville.....
 Pays.....
 email.....

svp – faites une photocopie de ce bon commande avant de le poster – svp parution mai 2018
 je commande..... exemplaire(s) du livre Survivrons-nous à la technologie
 au prix unitaire de 22 euros (franco de port)
Total =..... euros (franco de port)
que je règle par chèque bancaire joint à ce courrier et libellé à l'ordre de
Saint-Léger productions, 1, chemin des pièces Bron 49260 Le Coudray-Macouard
 ou par virement bancaire IBAN FR76 1027 8394 3700 0217 0820 246

II. Quelques ouvrages papiers relatifs au colloque de 2014 " Systèmes stellaires et planétaires- Conditions d'apparition de la Vie" - restent encore disponibles:

- Prix de l'ouvrage :25€.
- Pour toute commande s'adresser à Edith Perrier (voir coordonnées ci-dessus):

L'ouvrage cité ci-dessus est accessible gratuitement (open access) sur le site d'edp sciences:

<http://www.edp-open.org/images/stories/books/fulldl/Formation-des-systemes-stellaires-et-planetaires.pdf>

Documents

Pour préparer la conférence du Pr Gilles MONTAMBAUX sur " Transport Electronique quantique", nous vous proposons:

p. 08 : un résumé en français de sa présentation

p. 09 : issu du site <https://www.equipes.lps.u-psud.fr/Montambaux/polytechnique/PHY560B/copie-papier/papier-web-2017/PHY560B-Montambaux-01-06janvier2017.pdf> un article intitulé "Conduction quantique et Physique mésoscopique"

P. 21 issu du site https://www.researchgate.net/publication/249332328_Mesoscopic_physics_of_photons un article intitulé "Mesoscopic Physics of Photons" paru en janvier 2004 dans [Journal of the Optical Society of America B](#) 21

Transport électronique quantique par Gilles MONTAMBAUX

Résumé :

La miniaturisation des circuits électroniques et le développement des nanotechnologies ont permis de mettre en lumière de nouveaux effets quantiques régissant le transport électrique. Ces phénomènes apparaissent à une échelle intermédiaire entre l'échelle macroscopique de notre vie quotidienne et l'échelle atomique, nanoscopique. On appelle ceci l'univers mésoscopique. La physique mésoscopique se développe au croisement de deux nouvelles problématiques à la fois appliquées et conceptuelles. Le caractère quantique des électrons qui se comportent comme des ondes devient essentiel: Nous décrivons ici ces nouveaux effets dans lesquels la combinaison des rôles de cohérence de phase et de désordre conduit à des effets subtils. Il devient difficile de séparer l'objet quantique à étudier et l'univers macroscopique qui le mesure. Ces nouvelles propriétés ne sont pas propres aux électrons, mais elles se manifestent également dans la propagation d'autres ondes telles que la lumière, les micro-ondes, l'acoustique etc. Les analogies entre ces différents domaines thématiques sont fructueuses.

See discussions, stats, and author profiles for this publication at: <https://www.researchgate.net/publication/249332328>

Mesoscopic physics of photons

Article in *Journal of the Optical Society of America B* · January 2004

DOI: 10.1364/JOSAB.21.000101

CITATIONS

19

READS

28

2 authors:



[Eric Akkermans](#)

Technion - Israel Institute of Technology

92 PUBLICATIONS 2,931 CITATIONS

[SEE PROFILE](#)



[Gilles Montambaux](#)

Université Paris-Sud 11

178 PUBLICATIONS 5,493 CITATIONS

[SEE PROFILE](#)

Mesoscopic physics of photons

Eric Akkermans

Department of Physics, Technion, 32000 Haifa, Israel

Gilles Montambaux

Laboratoire de Physique des Solides, Université Paris-Sud, F-91405 Orsay Cedex, France

Received May 2, 2003; revised manuscript received July 31, 2003; accepted August 5, 2003

We review the general features of coherent multiple scattering of electromagnetic waves in random media. In particular, coherent backscattering and angular correlation functions of speckle patterns are studied in some detail. We present a general formalism based on a physically intuitive description that also permits us to derive quantitative expressions. Then, the notion of phase boxes describing the quantum crossings of diffusions is discussed. This notion permits us to understand the long-range correlations that are at the origin of most of the mesoscopic effects either for electrons or photons. Then, we turn to the problem of decoherence, namely, the washing out of interference effects. We use as an example the effect of a nondeterministic motion of the scatterers. We discuss some applications of these ideas to diffusive wave spectroscopy, including calculations of the intensity–time correlation function in the presence of quantum crossings. © 2004 Optical Society of America

OCIS codes: 290.4210, 030.5620, 030.1640, 030.6140.

1. INTRODUCTION

It has been widely accepted since the beginning of the 20th century that interference effects hardly survive multiple scattering. The success of powerful descriptions such as the radiative transfer equation for electromagnetic waves in random media or the Drude theory for metals is a consequence of this observation.

Nevertheless, such a statement is not entirely correct, and residual interference effects such as weak localization, the Sharvin–Sharvin effect, or the universal conductance fluctuations, have been proposed and observed first in metals. They have led to a completely new understanding of transport and thermodynamic properties of disordered metals and semiconductors. This new picture defines, as a whole, the field of mesoscopic quantum physics.^{1–4} The same reformulation also took place in the field of coherent multiple scattering of light,^{5–7} and the purpose of the present contribution is to review the mesoscopic physics of photons.

The study of interference effects in multiple scattering is an interesting subject on its own. The phenomenon is the basis of a large range of problems of interest such as the propagation of photons in cold atomic gases, suspensions of classical scatterers, and random lasers, to mention a few. The localization of light is a hotly debated and still unsolved problem. Unlike electrons, it is not possible to trap light (at least for the usual case of materials with positive dielectric function) in a potential well. The only remaining possibility is to achieve the Anderson localization transition through coherent multiple scattering. This is an additional strong incentive to study this problem.

2. COHERENCE AND MULTIPLE SCATTERING

We start with some elementary aspects of interference effects. To illustrate our approach, consider first the Young interferometer. A monochromatic wave emitted from a point source impinges on a screen with two parallel slits. The two emerging waves give rise to an interference pattern on a second screen placed far away. This pattern can often be seen with the unaided eye. It consists of a set of parallel bright fringes that result from the superposition of amplitudes whose length difference (in units of the wavelength) is an integer. The simplest way of predicting the form of the interference pattern is to ignore the vector character of the electromagnetic field and introduce a scalar electric field $E(\mathbf{r}, t)$. This amounts to ignoring polarization effects.

This interference pattern is very sensitive to any kind of dephasing. Suppose, for instance, that the source field $E(\mathbf{r}, t)$ is no longer monochromatic. It can then be written as a random Fourier superposition of orthogonal modes of different frequencies. The randomness accounts for the statistical uncertainty that characterizes the source. For stationary fields, the ensemble average can be replaced by a time average. The interference term in the intensity is now multiplied by the correlation function of the electric field $\langle E(\mathbf{r}, t)E^*(\mathbf{r}, t') \rangle$, and, following Born and Wolf,⁸ we define the degree of coherence at a point by

$$\gamma_{12}(\mathbf{r}, T) = \frac{\langle E(\mathbf{r}, T)E^*(\mathbf{r}, 0) \rangle}{\langle |E(\mathbf{r}, 0)|^2 \rangle}. \quad (1)$$

This function decreases with a characteristic phase coherence time T^* that describes the coherence of the source. The condition for observing interferences is that the length difference Δl between the two amplitudes is shorter than cT^* . It can be shown that the visibility of the fringes is directly proportional to $|\gamma_{12}(T = \Delta l/c)|$. If $|\gamma_{12}(\Delta l/c)| = 1$ the intensity at a point of the screen is the same as would be obtained with a strictly monochromatic light. In that case, we say that the two amplitudes that superpose are coherent. In the other limiting case, $|\gamma_{12}(\Delta l/c)| = 0$, the intensity is the sum of the intensities coming from the two slits, there is no longer any interference, and the superposition of the two waves is said to be incoherent. In the intermediate case, we shall speak of a partially coherent superposition. These general definitions apply not only to the Young interferometer, but to any kind of superposition of amplitudes or of intensities, such as in the Handbury-Brown-Twiss interferometer.⁹ To summarize, for time T smaller than the phase-coherence time, the coherence is maintained and the interference pattern is visible. For time T larger than the phase coherence time, the coherence is lost and the intensity at a point is simply the incoherent sum of the intensities.

Let us see now how this scheme can be extended to the case of multiple scattering in a stationary random medium. To that purpose we consider a monochromatic electromagnetic wave incident from a source placed outside the medium that experiences a large number of elastic scatterings in the medium before emerging and being collected on a detector placed far from the medium. We shall assume that the scatterings are independent, random events, each characterized by a scattering cross section σ . The elastic mean free path, defined by $l_e = 1/n_i\sigma$, where n_i is the density of scatterers, is the average distance between two successive scatterings. It is important to emphasize that l_e is much larger than the average distance $n_i^{-1/d}$ between scatterers, and it depends on the scattering properties of the potential through its cross section σ . For the sake of simplicity, the more general situation of anisotropic scattering and the distinction between elastic and transport mean free paths will not be considered here.^{5,7}

We consider the geometry of a slab (Fig. 1) for which the light incident from a source placed outside the medium scatters inside the medium and emerges either in reflection or in transmission. For a fixed configuration of scatterers, the image obtained on a screen is a speckle pattern which corresponds to the random superposition of

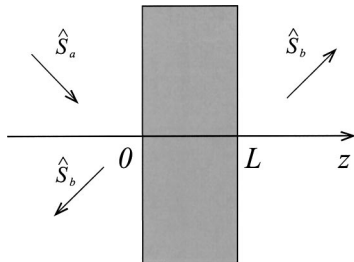


Fig. 1. Geometry of a slab of width L and section S used for the measurement of the angular-correlation functions both in reflection and in transmission.

the complex multiple scattering amplitudes. As such, the random distribution of bright and dark spots is analogous to the fringe pattern obtained in the Young interferometer, and the system is fully coherent. By averaging over the configurations, the interference pattern disappears. For a stationary, random distribution of moving scatterers, the equivalence between the configuration and the time averages relies on the ergodic assumption. In contrast to the Young interferometer, there are now two possibilities for decoherence. One might result from the source that emits light with a finite phase-coherence time. This corresponds to the situation of a partially coherent light discussed previously.

The other source of decoherence is the scattering medium itself. For instance, a nondeterministic motion of the scatterers will modify the speckle pattern.¹⁰⁻¹² Another example is provided by scatterers with internal degrees of freedom such as atomic degenerate levels.^{13,14} The characteristics of the photons emitted by these atoms (like resonant Rayleigh scattering) depend on the internal quantum states. The outgoing light is averaged over the statistical distribution of the atoms. This leads to a finite phase-coherence time that also modifies the interference pattern. It is usual, in the field of coherent multiple scattering, to discuss separately these two cases of decoherence. Here, we shall consider only situations where the decoherence originates from the scattering system itself and not from the properties of the source. We define a phase-coherence time τ_ϕ or, equivalently, a phase-coherence length L_ϕ . For a size L of the scattering system that is smaller than L_ϕ , coherence is preserved. This defines the mesoscopic regime, following the expression coined for electronic systems. For system sizes $L > L_\phi$, the system becomes incoherent and can be described classically.

The paper is organized as follows. The basic description of incoherent elastic multiple scattering is given in Section 3. The main quantity that permits us to describe the transport of the intensity is called the diffuson. It is obtained from a semiclassical description of multiple scattering, and it is equivalent to the solution of the radiative transfer equation.⁵ The diffuson is a classical object, thus insensitive to any dephasing process in the system. Among the various interference effects, we shall study first coherent backscattering, which modifies the average intensity reflected from a random medium. We shall proceed further with a description of the correlation properties of speckle patterns. They result from the random superposition of the multiple-scattered waves and can be viewed as a fingerprint of the corresponding disorder configuration. The bright or dark spots in those patterns have short-range correlations already present in the single scattering limit. They also exhibit long-range correlations that are a consequence of coherent multiple scattering.

3. MULTIPLE SCATTERING: DIFFUSON AND COOPERON

We turn now to a more quantitative description of interference effects in the multiple-scattering regime. Let us start with the following general setup. Consider a given

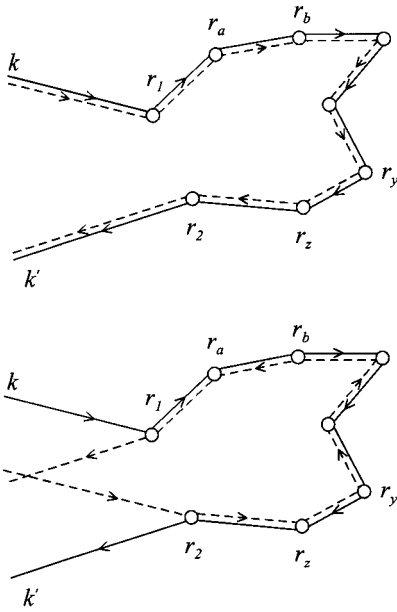


Fig. 2. Multiple scattering trajectories that contribute both to the incoherent and the coherent intensity.

configuration of scatterers (Fig. 2) and the corresponding amplitude $A(\mathbf{k}, \mathbf{k}')$ of a monochromatic plane wave of wavelength λ incident along the direction defined by the wave vector \mathbf{k} and outgoing along \mathbf{k}' . The amplitude can be written as

$$A(\mathbf{k}, \mathbf{k}') = \sum_{\mathbf{r}_1, \mathbf{r}_2} f(\mathbf{r}_1, \mathbf{r}_2) \exp[i(\mathbf{k} \cdot \mathbf{r}_1 - \mathbf{k}' \cdot \mathbf{r}_2)], \quad (2)$$

where $f(\mathbf{r}_1, \mathbf{r}_2)$ is the complex amplitude for the wave propagation between \mathbf{r}_1 and \mathbf{r}_2 and can be written as the sum $\sum_j a_j \exp(2i\pi\delta_j)$, where each path j represents a scattering sequence between the points \mathbf{r}_1 and \mathbf{r}_2 . The corresponding intensity is

$$\begin{aligned} |A(\mathbf{k}, \mathbf{k}')|^2 &= \sum_{\mathbf{r}_1, \mathbf{r}_2} \sum_{\mathbf{r}_3, \mathbf{r}_4} f(\mathbf{r}_1, \mathbf{r}_2) f^*(\mathbf{r}_3, \mathbf{r}_4) \\ &\quad \times \exp[i(\mathbf{k} \cdot \mathbf{r}_1 - \mathbf{k}' \cdot \mathbf{r}_2)] \\ &\quad \times \exp[-i(\mathbf{k} \cdot \mathbf{r}_3 - \mathbf{k}' \cdot \mathbf{r}_4)] \end{aligned} \quad (3)$$

with

$$\begin{aligned} f(\mathbf{r}_1, \mathbf{r}_2) f^*(\mathbf{r}_3, \mathbf{r}_4) &= \sum_{j, j'} a_j^*(\mathbf{r}_1, \mathbf{r}_2) a_{j'}(\mathbf{r}_3, \mathbf{r}_4) \\ &= \sum_{j, j'} |a_j| |a_{j'}| \exp[2i\pi(\delta_{j'} - \delta_j)]. \end{aligned} \quad (4)$$

The phase $\delta_{j'} - \delta_j$ measures the length difference between multiple-scattering trajectories in units of the wavelength λ . Except for identical scattering sequences, this difference is always comparable with the elastic mean free path l_e . In the weak scattering (or weak disorder) regime defined by $l_e \gg \lambda$, this phase difference is a rapidly oscillating function. Therefore, on average over

the configurations, most of the contributions to the intensity disappear except those corresponding to identical scattering sequences.

For a given scattering sequence, there are two choices for the corresponding identical sequence: either passing through the same sequence of scatterers or passing through them but in reversed order (Fig. 2). Moreover, to have identical trajectories imposes that $\mathbf{r}_1 = \mathbf{r}_3$ and $\mathbf{r}_2 = \mathbf{r}_4$ in Eq. (3) for the first choice, and $\mathbf{r}_1 = \mathbf{r}_4$ and $\mathbf{r}_2 = \mathbf{r}_3$ for the second. We thus obtain for the average intensity

$$\begin{aligned} \overline{|A(\mathbf{k}, \mathbf{k}')|^2} &= \sum_{\mathbf{r}_1, \mathbf{r}_2} \overline{|f(\mathbf{r}_1, \mathbf{r}_2)|^2} \\ &\quad \times \{1 + \exp[i(\mathbf{k} + \mathbf{k}') \cdot (\mathbf{r}_1 - \mathbf{r}_2)]\}. \end{aligned} \quad (5)$$

The second term in the curly brackets contains a phase factor that depends on the two points \mathbf{r}_1 and \mathbf{r}_2 . The sum over those points makes this term vanishing except for two remarkable cases:

1. $\mathbf{k} + \mathbf{k}' \approx 0$; for an outgoing direction exactly opposite to the incident one, the intensity is exactly twice its classical (incoherent) value. Moreover, since the classical expression does not involve any angular dependence, the second term that depends on $\mathbf{k} + \mathbf{k}'$ gives a peak to the average reflected intensity. This phenomenon is called coherent backscattering.^{15,16} It is the last interference effect that, for weak scattering, survives the disorder average.

2. In the sum of Eq. (5), terms such that $\mathbf{r}_1 = \mathbf{r}_2$ are peculiar since they describe closed trajectories. It is a coherent contribution to the average that remains finite even if it is not possible to keep the directions \mathbf{k} and \mathbf{k}' fixed. This is the case in metals or semiconductors where this coherent contribution modifies the average transport properties, such as the electrical conductivity. This term is at the origin of the weak localization phenomenon.

The second term in Eq. (5) describes the interference between two time-reversed trajectories. Its occurrence requires that the two reversed sequences see exactly the same scattering events. Therefore, any process that breaks this interference such as a nondeterministic motion of the scatterers, a trace over internal degrees of freedom, or a breaking of the time-reversal symmetry, to mention a few, will be a source of decoherence. As such, it will be described by a degree of coherence or by a phase-coherence time τ_ϕ . We shall come to this later on.

The incoherent and coherent contributions that appear in the average intensity Eq. (5) are called, respectively, diffuson and cooperon. The diffuson $\overline{|f(\mathbf{r}, \mathbf{r}')|^2}$ is given by the sum of all the scattering sequences, and it represents the classical probability of joining the points \mathbf{r} and \mathbf{r}' (see Fig. 3). It can be generalized to the case of two amplitudes taken at different frequencies ω_0 and $\omega_0 - \omega$, namely, $\overline{f_{\omega_0}(\mathbf{r}, \mathbf{r}') f_{\omega_0 - \omega}^*(\mathbf{r}', \mathbf{r})}$. More precisely, we define the probability

$$P(\mathbf{r}, \mathbf{r}', \omega) = \frac{4\pi}{c} \overline{f_{\omega_0}(\mathbf{r}, \mathbf{r}') f_{\omega_0 - \omega}^*(\mathbf{r}', \mathbf{r})}, \quad (6)$$

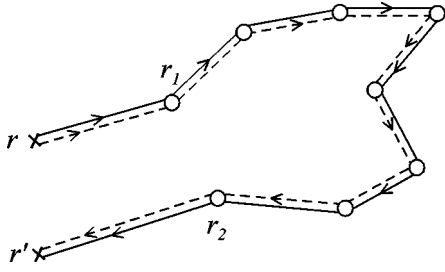


Fig. 3. Multiple scattering trajectories that contribute to the classical probability.

where c is the velocity of the wave.

This probability is normalized so that its Fourier transform obeys $\int_0^\infty d\mathbf{r}' P(\mathbf{r}, \mathbf{r}', t) = 1$.⁵ Further insights regarding the probability are given in Refs. 4, 5, and 7. Here we shall use only its expression in the limit of slow spatial and frequency variations, i.e., for $|\mathbf{r} - \mathbf{r}'| \gg l_e$ and $\omega\tau_e \ll 1$. It is then the solution of the diffusion equation

$$(-i\omega - D\Delta_{\mathbf{r}})P(\mathbf{r}, \mathbf{r}', \omega) = \delta(\mathbf{r} - \mathbf{r}'), \quad (7)$$

where the diffusion coefficient is defined by $D = cl_e/3 = l_e^2/(3\tau_e)$. The diffuson, or solution to Eq. (7), is long ranged. For instance, it behaves like $P(\mathbf{r}, \mathbf{r}') = 1/4\pi D|\mathbf{r} - \mathbf{r}'|$ in three-dimensional free space.

The behavior of the diffuson can also be obtained from the so-called radiative transfer equation, which gives the solutions of the specific intensity of the wave.⁵ This latter approach, which is strictly equivalent, is more systematic although less versatile. It permits one to implement physical boundary conditions for the diffuson by demanding that the diffusive flux incident on the scattering medium vanish. For the geometry of a slab (Fig. 1), this boundary condition corresponds to the vanishing of P outside the disordered slab at the points $-z_0$ and $L + z_0$ with $z_0 = (2/3)l_e$.

4. COHERENT BACKSCATTERING CONE

We now return to the coherent backscattering interference effect for the geometry of a semi-infinite disordered system (Fig. 4). A monochromatic wave emitted from a source placed at infinity is incident on the interface of surface S . It experiences multiple scattering before emerging and being collected on a detector placed far from the interface and defined by the direction $\hat{\mathbf{s}}_e$.

The reflected intensity, also called the albedo α , is given by the ratio between the flux of the Poynting vector per unit time and solid angle and the incident flux. Assuming that the incident light is perpendicular to the interface, we obtain for the average incoherent albedo α_d the following expression written in terms of the diffuson⁵:

$$\alpha_d = \frac{c}{4\pi l_e^2 S} \int d\mathbf{r}_1 d\mathbf{r}_2 \exp\left(-\frac{z_1}{l_e}\right) \exp\left(-\frac{z_2}{\mu l_e}\right) P(\mathbf{r}_1, \mathbf{r}_2), \quad (8)$$

where μ is the projection of $\hat{\mathbf{s}}_e$ along the z axis. For a semi-infinite medium, we obtain

$$\alpha_d = \frac{c}{4\pi l_e^2} \int_0^\infty dz_1 dz_2 \exp\left(-\frac{z_1}{l_e}\right) \times \exp\left(-\frac{z_2}{\mu l_e}\right) \int_S d^2\rho P(\rho, z_1, z_2). \quad (9)$$

The solution of the stationary ($\omega = 0$) diffuson Eq. (7) for this geometry and with the effective boundary condition derived from the radiative transfer equation is obtained by using the image method:

$$P(\rho, z_1, z_2) = \frac{1}{4\pi D} \left[\frac{1}{\sqrt{\rho^2 + (z_1 - z_2)^2}} - \frac{1}{\sqrt{\rho^2 + (z_1 + z_2 + 2z_0)^2}} \right], \quad (10)$$

with $z_0 = \frac{2}{3}l_e$. The incoherent albedo is thus given by

$$\alpha_d = \frac{3}{4\pi} \mu \left(\frac{z_0}{l_e} + \frac{\mu}{\mu + 1} \right). \quad (11)$$

It depends very weakly on the angle between the ingoing and the outgoing directions.

The coherent contribution α_c is similarly obtained^{17,18} from relation (5) so that

$$\alpha_c = \frac{c}{4\pi l_e^2} \int d\mathbf{r}_1 d\mathbf{r}_2 \exp\left[-\left(\frac{\mu + 1}{2\mu}\right) \frac{z_1 + z_2}{l_e}\right] P(\mathbf{r}_1, \mathbf{r}_2) \times \exp[ik(\hat{\mathbf{s}}_i + \hat{\mathbf{s}}_e) \cdot (\mathbf{r}_2 - \mathbf{r}_1)]. \quad (12)$$

The phase factor accounts for the angular dependence of the coherent albedo. In the backscattering direction $\hat{\mathbf{s}}_i + \hat{\mathbf{s}}_e = 0$, we have (Fig. 5)

$$\alpha_c(\theta = 0) = \alpha_d. \quad (13)$$

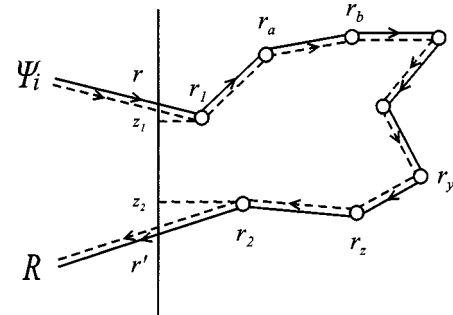


Fig. 4. Contribution of the diffuson to the average incoherent albedo.

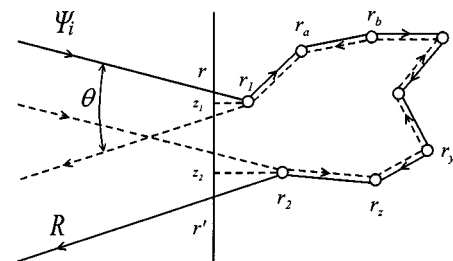


Fig. 5. Contribution of the cooperon to the average coherent albedo.

By defining the projection $\mathbf{k}_\perp = (\mathbf{k}_i + \mathbf{k}_e)_\perp = k(\hat{\mathbf{s}}_i + \hat{\mathbf{s}}_e)_\perp$ onto the interface and considering the limit of small angles, we can disregard the projection of $\hat{\mathbf{s}}_i + \hat{\mathbf{s}}_e$ onto the $O-z$ axis,¹⁹ so that the coherent albedo may be rewritten

$$\alpha_c = \frac{c}{4\pi l_e^2} \int_0^\infty dz_1 dz_2 \times \exp\left[-\left(\frac{\mu+1}{2\mu}\right)\frac{z_1+z_2}{l_e}\right] \times \int_S d^2\rho P(\rho, z_1, z_2) \exp(i\mathbf{k}_\perp \cdot \boldsymbol{\rho}). \quad (14)$$

The second integral is nothing but the Fourier transform $P(k_\perp, z_1, z_2)$ of $P(\rho, z_1, z_2)$ given by Eq. (10):

$$P(k_\perp, z_1, z_2) = \frac{1}{2Dk_\perp} \{\exp(-k_\perp|z_1 - z_2|) - \exp[-k_\perp(z_1 + z_2 + 2z_0)]\}. \quad (15)$$

Neglecting the weak μ dependence, we obtain

$$\alpha_c(\theta) = \frac{3}{8\pi} \frac{1}{(1+k_\perp l_e)^2} \left[1 + \frac{1 - \exp(-2k_\perp z_0)}{k_\perp l_e} \right]. \quad (16)$$

For small angles, $k_\perp \approx (2\pi/\lambda)\theta$, the coherent albedo is nonvanishing within a cone of angular width $\lambda/2\pi l_e$ around the backscattering direction, and

$$\alpha_c(\theta) \approx \alpha_c(0) - \frac{3}{4\pi} \frac{(l_e + z_0)^2}{l_e} k_\perp + O(k_\perp^2). \quad (17)$$

We use the notation

$$\alpha_c(\theta) \approx \alpha_c(0) - \beta k_\perp l_e, \quad (18)$$

with

$$\beta = \frac{3}{4\pi} \left(1 + \frac{z_0}{l_e} \right)^2 = \frac{25}{12\pi}. \quad (19)$$

The coherent backscattering peak has a cusp singularity which results from the sum of the coherent contributions of all the possible multiple scattering paths. This behavior has been observed in great detail.²⁰⁻²³ To obtain further insight, we write the probability under the form $P(k_\perp, z, z') = \int_0^\infty dt P(k_\perp, z, z', t)$ where

$$P(k_\perp, z, z', t) = \frac{\exp(-Dk_\perp^2 t)}{(4\pi Dt)^{1/2}} \{\exp[-(z - z')^2/4Dt] - \exp[-(z + z' + 2z_0)^2/4Dt]\}. \quad (20)$$

Here, the time parameter t plays the role of the length n of the diffusion path, namely, $t = n\tau_e$. For long enough trajectories, $t \gg \tau_e$, we have

$$\alpha_c(\theta) \approx \frac{25}{9} c l_e^2 \int_0^\infty dt \frac{\exp(-Dk_\perp^2 t)}{(4\pi Dt)^{3/2}}. \quad (21)$$

The coherent albedo thus appears as a sum of Gaussian terms weighted by the probability $(Dt)^{-3/2}$ for a random

walk to reach the plane $z = z_0$. While each term is parabolic around $\theta = 0$, the integral has a singularity around this value. The angle θ appears as the conjugate of the length $n = t/\tau_e$ of the diffuson paths. Hence, the contribution at small angle results from the long multiple-scattering trajectories. In the presence of a finite phase-coherence length L_ϕ , the trajectories longer than L_ϕ are no longer coherent and therefore do not contribute to the coherent backscattering peak, which appears rounded off at small angles.

5. CORRELATIONS IN SPECKLE PATTERNS

Thus far, we have studied the behavior of the average intensity. The ensemble average is obtained by assuming ergodicity and by using either the rotation of a solid sample or the motion of the scatterers. In the latter case, an incident wave packet (a pulse) probes a static configuration of the scatterers. This is a consequence of the large ratio between the velocities of the light and of the scatterers. Hence, a pulse realizes an instantaneous picture of the disordered medium known as a speckle pattern that displays a random distribution of bright and dark spots. More quantitatively, the intensity distribution is shown to obey a Rayleigh law that states that the fluctuations are large and of the order of the average intensity.

A broad range of measurements can be performed on speckle patterns. An example is provided by the angular-correlation function. For the slab geometry of Fig. 1, an incident beam along the direction $\hat{\mathbf{s}}_a$ is either reflected or transmitted along $\hat{\mathbf{s}}_b$. The transmission coefficient \mathcal{T}_{ab} is defined just like the albedo, i.e., by the flux of the Poynting vector along the outgoing direction per unit time and solid angle, normalized to the incident flux. It is important to take into account that this geometry differs from the waveguide geometry generally used to describe the conductance of a conductor within the Landauer formalism. In this latter case, the incident and transmitted waves are plane waves with boundary conditions imposed by the waveguide. This leads to the quantization of the transverse channels. Here, instead, there are incident plane waves but transmitted spherical waves. This corresponds to different boundary conditions and to a continuous distribution of the transmitted angular directions.⁵

To go further, we consider the normalized correlation function

$$C_{aba'b'} = \frac{\overline{\delta\mathcal{T}_{ab}\delta\mathcal{T}_{a'b'}}}{\overline{\mathcal{T}_{ab}\mathcal{T}_{a'b'}}}, \quad (22)$$

where $\delta\mathcal{T}_{ab} = \mathcal{T}_{ab} - \overline{\mathcal{T}_{ab}}$.

By definition, this correlation function is obtained from the product of four complex amplitudes (Fig. 6) describing multiple-scattering sequences in the disordered medium. Here again, as for the average intensity, the nonvanishing contributions correspond to the amplitudes that can be paired into diffusons (Fig. 7).

For the angular configuration $a = a'$ and $b = b'$, the two contributions of Fig. 7 are identical and we obtain

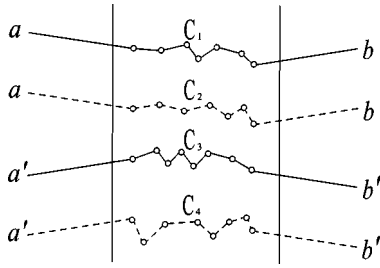


Fig. 6. Angular-correlation function in transmission corresponding to four waves incident along the directions $\hat{\mathbf{s}}_a$ and $\hat{\mathbf{s}}_{a'}$ and outgoing along the directions $\hat{\mathbf{s}}_b$ and $\hat{\mathbf{s}}_{b'}$. A nonzero contribution corresponds to the pairing of two amplitudes into a diffusion.

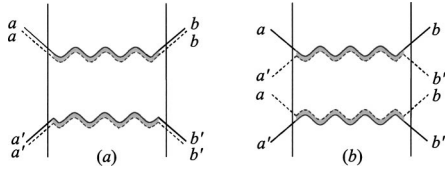


Fig. 7. Two contributions to the product $\overline{\mathcal{T}_{ab}\mathcal{T}_{a'b'}}$, that correspond, respectively, to the pairing $C_1 = C_2$, $C_3 = C_4$ and $C_1 = C_4$, $C_2 = C_3$. The first gives $\overline{\mathcal{T}_{ab}\mathcal{T}_{a'b'}}$. The second corresponds to the angular correlation function noted $C_{aba'b'}^{(1)}$ in the text.

$$\overline{\delta\mathcal{T}_{ab}^2} = \overline{\mathcal{T}_{ab}^2}. \quad (23)$$

This constitutes the Rayleigh law that accounts for the characteristic granular structure of a speckle pattern, i.e., relative fluctuations of order unity. This is the most important and “visible” property of a speckle pattern. It exists also in the single-scattering regime.²⁴

The average transmission coefficient $\overline{\mathcal{T}_{ab}}$ involves one diffuson. Its calculation is analogous to the one leading to the incoherent albedo α_d . It should be noted that in transmission there is obviously no coherent backscattering effect, but there are weak localization effects that we do not consider. In the slab geometry and similar to expression (8), we have

$$\overline{\mathcal{T}_{ab}} = \frac{c}{4\pi l_e^2} \int dz_1 dz_2 d^2\rho \exp(-z_1/\mu_a l_e) \times \exp(-|L - z_2|/\mu_b l_e) P(\rho, z_1, z_2), \quad (24)$$

where μ_a (resp. μ_b) is the projection of $\hat{\mathbf{s}}_a$ (resp. $\hat{\mathbf{s}}_b$) along the z axis. Integrating over z_1 and z_2 , we obtain

$$\begin{aligned} \overline{\mathcal{T}_{ab}} &= \frac{c}{4\pi} \mu_a \mu_b \int_S d^2\rho P(\rho, \mu_a l_e, L - \mu_b l_e) \\ &= \frac{c}{4\pi} \mu_a \mu_b P(k_\perp = 0, \mu_a l_e, L - \mu_b l_e), \end{aligned} \quad (25)$$

which involves the two-dimensional Fourier transform of the diffusion that in the slab geometry is

$$P(k_\perp, z, z') = \frac{1}{D} \frac{\sinh k_\perp z_m \sinh k_\perp (L - z_M)}{k_\perp \sinh k_\perp L}, \quad (26)$$

with $z_m = \min(z, z')$ and $z_M = \max(z, z')$. For $k_\perp = 0$ we have

$$P(0, z, z') = \frac{z_m}{D} \left(1 - \frac{z_M}{L}\right). \quad (27)$$

By inserting this relation into Eq. (25), we obtain for small angles $\mu_a \approx \mu_b \approx 1$

$$\overline{\mathcal{T}_{ab}} = \frac{3}{4\pi} \frac{l_e}{L}. \quad (28)$$

This relation results from a particular choice of boundary conditions for the diffusion equation, namely, a vanishing of the probability at the boundaries $z = 0, L$ of the slab. We have seen that a more precise calculation should use the extrapolation length $z_0 = \frac{2}{3}l_e$ so that $z_m \rightarrow z_m + z_0$ and $z_M \rightarrow z_M + z_0$ in Eq. (27). This is of no importance for the calculation of the normalized correlation function of Eq. (22).

A. Short-Range Correlation $C^{(1)}$

The main contribution to the angular-correlation function is shown by Fig. 7(b). Its calculation is very similar to those of the average transmission coefficient apart from the additional phase factors.²⁵ By defining the vectors $\Delta\hat{\mathbf{s}}_a = \hat{\mathbf{s}}_a - \hat{\mathbf{s}}_{a'}$ and $\Delta\hat{\mathbf{s}}_b = \hat{\mathbf{s}}_b - \hat{\mathbf{s}}_{b'}$ and neglecting their projection along the z axis, we have

$$\begin{aligned} \overline{\delta\mathcal{T}_{ab}\delta\mathcal{T}_{a'b'}} &= \left\{ \frac{c}{4\pi l_e^2} \int d^2\rho dz_1 dz_2 \right. \\ &\quad \times \exp[ik(\Delta\hat{\mathbf{s}}_a \cdot \boldsymbol{\rho}_1 - \Delta\hat{\mathbf{s}}_b \cdot \boldsymbol{\rho}_2)] \exp(-z_1/l_e) \\ &\quad \left. \times \exp(-|L - z_2|/l_e) P(\rho, z_1, z_2) \right\}^2. \end{aligned} \quad (29)$$

By performing the z integrals and defining $q_a = k|\Delta\hat{\mathbf{s}}_a|$, we obtain for $q_a l_e \ll 1$,

$$C_{aba'b'}^{(1)} = \delta_{\Delta\hat{\mathbf{s}}_a, \Delta\hat{\mathbf{s}}_b} F_1(q_a L) = \delta_{\Delta\hat{\mathbf{s}}_a, \Delta\hat{\mathbf{s}}_b} \left(\frac{q_a L}{\sinh q_a L} \right)^2 \quad (30)$$

with

$$F_1(x) = \left(\frac{x}{\sinh x} \right)^2 \quad (31)$$

This expression permits us to understand some of the qualitative insights of the memory effect.^{26,27,19}

The structure of expression (29) is formally similar to expression (14) for the coherent albedo. To make this analogy more quantitative, consider the correlation function of the reflection coefficient \mathcal{R}_{ab} defined by

$$\begin{aligned} \overline{\delta\mathcal{R}_{ab}\delta\mathcal{R}_{a'b'}} &= \left\{ \frac{c}{4\pi l_e^2} \int d^2\rho dz_1 dz_2 \right. \\ &\quad \times \exp[ik(\Delta\hat{\mathbf{s}}_a \cdot \mathbf{r}_1 - \Delta\hat{\mathbf{s}}_b \cdot \mathbf{r}_2)] \exp(-z_1/l_e) \\ &\quad \left. \times \exp(-z_2/l_e) P(\rho, z_1, z_2) \right\}^2, \end{aligned} \quad (32)$$

which we may rewrite as

$$\overline{\delta\mathcal{R}_{ab}\delta\mathcal{R}_{a'b'}} = \delta_{\Delta\hat{s}_a, \Delta\hat{s}_b} \left[\frac{c}{4\pi l_e^2} \int_0^\infty dz_1 dz_2 \exp(-z_1/l_e) \right. \\ \left. \times \exp(-z_2/l_e) P(q_a, z_1, z_2) \right]^2, \quad (33)$$

where $q_a = k|\Delta\hat{s}_a|$. Using expression (14) of the coherent albedo, we then have

$$\overline{\delta\mathcal{R}_{ab}\delta\mathcal{R}_{a'b'}} = \bar{\mathcal{R}}_{ab}\bar{\mathcal{R}}_{a'b'} \delta_{\Delta\hat{s}_a, \Delta\hat{s}_b} \left[\frac{\alpha_c(q_a)}{\alpha_c(0)} \right]^2. \quad (34)$$

B. Diffuson Crossings: Phase Box and Long-Range Correlations

Until now, we have managed to reduce a given product of complex amplitudes to a product of diffusons (or cooperons for the coherent albedo). The diffuson is a classical solution independent of the phases of the two underlying complex amplitudes. There is nevertheless a way to retrieve information about these phases when two diffusons cross each other or at the self-crossing of a single diffuson. To get some further insight, we consider the situation depicted in Fig. 8. There, the two ingoing diffusons exchange their complex amplitudes to build two outgoing diffusons in which the amplitudes are paired differently. To preserve the coherence at a crossing, we must require that its spatial extension not exceed the elastic mean free path l_e so as not to accumulate too large a phase mismatch. It can be shown that the volume of such a ‘‘phase box’’ is $\lambda^2 l_e$.⁵ We shall characterize the phase box in more detail in Subsection 5.C. We just mention here that these phase boxes, also called Hikami boxes in the literature, play a ubiquitous role in mesoscopic quantum physics.^{28–31}

Since a phase box preserves the coherence and exchanges complex amplitudes, a diffuson crossing can be viewed as an interference effect. It is therefore important to evaluate the occurrence of such crossings. To that purpose, we consider again the geometry of a slab of width L and volume $\Omega = LS$, where the characteristic time for a diffusive trajectory to transit the sample is τ_D

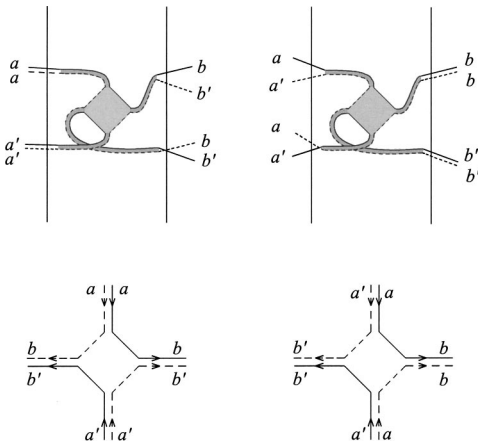


Fig. 8. Contribution to $\overline{\delta\mathcal{T}_{ab}\delta\mathcal{T}_{a'b'}}$ involving one crossing of the two diffusons. The different cases correspond to configurations of plane waves incident along \hat{s}_a and $\hat{s}_{a'}$, and outgoing along \hat{s}_b and $\hat{s}_{b'}$. The diagrams on the left depend on $\Delta\hat{s}_b$ but not on $\Delta\hat{s}_a$ and the opposite for the diagrams on the right.

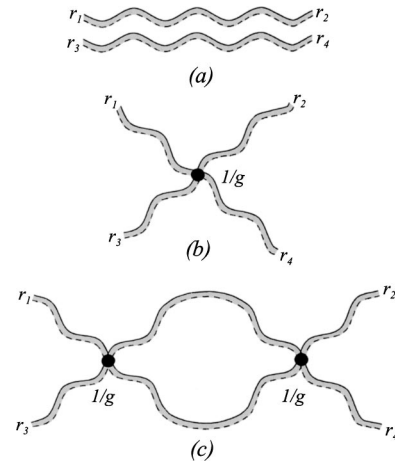


Fig. 9. Classification of the contributions to the correlation-function $C_{aba'b'}$ in terms of the number of crossings of two diffusons. At each crossing, the corresponding contribution is multiplied by $1/g \ll 1$. The three contributions represented in (a), (b), (c) are denoted, respectively, $C^{(1)}$, $C^{(2)}$, $C^{(3)}$.

$= L^2/D$. The length of this trajectory is thus $\mathcal{L} = c\tau_D = 3L^2/l_e$. The volume of the crossing being $\lambda^2 l_e$, we may characterize a diffuson by its length \mathcal{L} and its cross section λ^2 . The occurrence of a crossing is thus given by the ratio of the two volumes $\lambda^2 \mathcal{L}/\Omega = \lambda^2 L/l_e S \propto 1/g$, where we have defined the dimensionless quantity

$$g = \frac{k^2 l_e S}{3\pi L}, \quad (35)$$

with $k = 2\pi/\lambda$. This is the so-called dimensionless conductance of a wire of length L and section S . In the limit $kl_e \gg 1$ of a weak disorder, g is large, typically of the order of 10^2 . Therefore, we may assume that the crossing events are uncorrelated, so that the probability of n crossings is given by $1/g^n$. This permits us to classify any contribution in terms of its number of crossings as represented in Fig. 9.

The contributions to the average intensity, as with the albedo, may also involve one or more self-crossings. This is at the origin of the so-called weak localization corrections and, more generally, the scaling theory of the Anderson localization transition.

For the case of the speckle correlation functions, we have additional contributions involving one or more crossings. We shall now study them.

C. Long-Range Correlations $C^{(2)}$ and $C^{(3)}$

The next contribution to the correlation function arises from terms involving one crossing of two diffusons (Fig. 8). Because of the structure of the phase box the angular-correlation function is different from $C^{(1)}$. This gives rise to the two possibilities

$$(aa)(a'a') \rightarrow (bb')(bb') \quad (36)$$

and

$$(aa')(aa') \rightarrow (bb)(b'b'). \quad (37)$$

The corresponding expression for these two cases is

$$\begin{aligned} \overline{\delta\mathcal{T}_{ab}\delta\mathcal{T}_{a'b'}}^{(2)} &= \left(\frac{c}{Sl_e^2}\right)^2 \int \prod_{i=1}^4 d\mathbf{r}_i \{ \exp[ik\Delta\hat{\mathbf{s}}_b \cdot (\mathbf{r}_2 - \mathbf{r}_4)] \\ &\quad + \exp[ik\Delta\hat{\mathbf{s}}_a \cdot \Delta(\mathbf{r}_1 - \mathbf{r}_3)] \} E(z_i) \\ &\quad \times \int \prod_{i=1}^4 d\mathbf{R}_i H(\mathbf{R}_i) P(\mathbf{r}_1, \mathbf{R}_1) P(\mathbf{r}_3, \mathbf{R}_3) \\ &\quad \times P(\mathbf{R}_2, \mathbf{r}_2) P(\mathbf{R}_4, \mathbf{r}_4), \end{aligned} \quad (38)$$

where $H(\mathbf{R})$ accounts for the Hikami phase box describing the crossing of the two diffusons. It is given by^{5,7,26,29}

$$H(\mathbf{r}_1, \mathbf{r}_2, \mathbf{r}_3, \mathbf{r}_4) = \frac{l_e^5}{24\pi k^2} \int d\mathbf{r} \prod_{i=1}^4 \delta(\mathbf{r} - \mathbf{r}_i) \nabla_2 \cdot \nabla_4, \quad (39)$$

where we have defined

$$\begin{aligned} E(z_i) &= \exp[-(z_1 + z_3)/l_e] \\ &\quad \times \exp(-|L - z_2|/l_e) \exp(-|L - z_4|/l_e). \end{aligned} \quad (40)$$

The two gradients act on the incoming diffusons for the case of the diagrams on the left in Fig. 8 and on the outgoing diffusons for the diagrams on the right, and both give the same contribution. Performing the integrals over the z_i 's is equivalent to assuming that $z_1 = z_3 = l_e$ and $z_2 = z_4 = L - l_e$. Hence

$$\begin{aligned} \overline{\delta\mathcal{T}_{ab}\delta\mathcal{T}_{a'b'}}^{(2)} &= \frac{l_e c^4}{24\pi k^2 S} \int_0^L dz [\partial_z P(0, l_e, z)]^2 \\ &\quad \times P(q_b, z, L - l_e)^2, \end{aligned} \quad (41)$$

where, for the geometry of the slab, $P(q_b, z, z')$ is given by Eq. (26) with $q_b = k|\Delta\hat{\mathbf{s}}_b|$. Hence, in the limit $q_b l_e \ll 1$,

$$\partial_z P(0, l_e, z) = -\frac{l_e}{DL}, \quad P(q_b, z, L - l_e) = \frac{l_e \sinh q_b z}{D \sinh q_b L}, \quad (42)$$

so that

$$\overline{\delta\mathcal{T}_{ab}\delta\mathcal{T}_{a'b'}}^{(2)} = \frac{81}{48\pi} \frac{l_e}{k^2 L S} F_2(q_b L), \quad (43)$$

where we have defined

$$F_2(x) = \frac{1}{\sinh^2 x} \left(\frac{\sinh 2x}{2x} - 1 \right). \quad (44)$$

The total contribution of the two diagrams to the angular-correlation function is thus given at this order by^{5,29,31,32}

$$C_{aba'b'}^{(2)} = \frac{\overline{\delta\mathcal{T}_{ab}\delta\mathcal{T}_{a'b'}}}{\overline{\mathcal{T}_{ab}}^2} = \frac{1}{g} [F_2(q_a L) + F_2(q_b L)]. \quad (45)$$

The function $F_2(x)$ decreases like $1/x$ at infinity and not exponentially like the correlation function $C_{aba'b'}^{(1)}$ in the absence of diffuson crossings. For instance, the speckle pattern associated with an incident light such that a

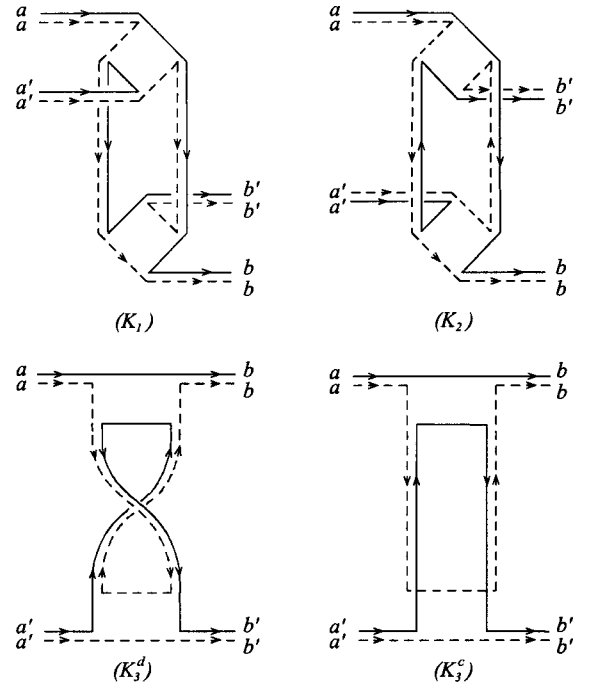


Fig. 10. Two crossings terms. Such diagrams do not give rise to an angular structure.

$= a'$ involves long-range angular correlations, but of weak amplitude proportional to $1/g$ that accounts for the crossing probability, namely

$$C_{abab'}^{(2)} = \frac{1}{g} \left(\frac{2}{3} + F_2(kL\Delta\hat{\mathbf{s}}_b) \right)^{b \neq b'} \frac{2}{3g} \quad (46)$$

A higher-order contribution in the expansion of the angular-correlation function in powers of $1/g$ involves two crossings and is represented in Fig. 10. It is easy to see that it does not involve any angular structure as a result of the pairing of the trajectories. The respective correlation function thus corresponds to the angular structure

$$C^{(3)}: (aa)(a'a') \rightarrow (bb)(b'b'). \quad (47)$$

To proceed further, we consider the case depicted by K_1 in Fig. 10. Its calculation is analogous to those leading to $C_{abab'}^{(2)}$, and we take the gradients in the two phase boxes as acting on the incoming and outgoing diffusons and not on the internal ones. We thus obtain

$$\begin{aligned} \overline{\delta\mathcal{T}_{ab}\delta\mathcal{T}_{a'b'}}^{(3)}|_{K_1} &= (2h_4)^2 \frac{l_e^4}{(4\pi)^4 S^2} \left(\frac{4\pi c}{l_e^2} \right)^4 \\ &\quad \times \int_0^L \int_a^L dz dz' [\partial_z P(0, l_e, z)]^2 \\ &\quad \times P(0, z, z')^2 [\partial_{z'} P(0, z', L - l_e)]^2, \end{aligned} \quad (48)$$

with $h_4 = l_e^5/48\pi k^2$, so that

$$C_{aba'b'}^{(3)}|_{K_1} = \frac{4}{g^2} \frac{D^2}{L^4} \int_0^L \int_0^L dz dz' P(z, z')^2. \quad (49)$$

Case K_2 in Fig. 10 gives an identical contribution, while K_3^d and K_3^c give each half of the K_1 contribution.⁵ Finally

$$C_{aba'b'}^{(3)} = \frac{\overline{\delta\mathcal{T}_{ab}\delta\mathcal{T}_{a'b'}}^{(3)}}{\bar{\mathcal{T}}_{ab}^2} = \frac{2}{15} \frac{1}{g^2}. \quad (50)$$

This expression is said to be universal in the sense that it does not depend on the elastic mean free path l_e , i.e., on the disorder. It is the equivalent of the well-known universal conductance fluctuations in electronic systems.^{33,34}

It is interesting to note that we have obtained an identical result using a different definition of the transmission coefficient, i.e., a different geometry where the conduction channels do not appear. This is true for the relative fluctuations but not for the second moment.

There are other contributions to the two-crossings term that have the angular structure of either $C^{(1)}$ or $C^{(2)}$. They correspond to higher-order terms in the $1/g$ expansion of the corresponding correlation functions.

The different contributions associated with the crossings of diffusons have been identified and measured.³⁵ We shall come back to this in Section 6.

6. DIFFUSIVE-WAVE SPECTROSCOPY: DECOHERENCE

In the previous sections, we have studied interference effects in the elastic multiple scattering of light in random systems. As such, the effects are very sensitive to the coherence properties in the system. We have discussed in the introduction various sources of decoherence. Here, we are not interested in the properties of the source and we assume that it emits coherent, monochromatic waves. Instead, we focus on the coherence properties of the scattering medium.

We have seen that the diffuson or the cooperon results from the pairing of two complex-conjugate amplitudes describing the same sequences of scattering events. A full-phase coherence is maintained as long as the two complex amplitudes that contribute to the diffuson and the cooperon remain in phase. If, on the other hand, a random source of dephasing affects differently the two conjugate scattering sequences, this will lead to a loss of coherence and to a washout of the interference effects.

To be more specific, we consider again the case of a non-deterministic motion of the scatterers. Then, following the discussion of the introduction, the degree of coherence at a point \mathbf{r} of the scalar electric field $E(\mathbf{r}, T)$ is given by the time-correlation function of Eq. (1). The electric field inside the scattering medium results from the superposition of all the multiple-scattering sequences:

$$E(\mathbf{r}, T) = \sum_{n=1}^{\infty} \sum_{C_n} |A[C_n(T)]| \exp[i\phi_n(T)], \quad (51)$$

where C_n is a sequence of n scatterings and where the phase $\phi_n(T)$ depends on the disorder configuration at time T . The degree of coherence may thus be expressed as

$$\begin{aligned} \gamma_{12}(\mathbf{r}, T) &\propto \sum_{n,n'} \sum_{C_n, C_{n'}} \langle |A[C_n(T)]| |A[C_{n'}(0)]| \\ &\times \exp\{i[\phi_n(T) - \phi_{n'}(0)]\}, \end{aligned} \quad (52)$$

where the notation $\langle \dots \rangle$ accounts for the average over the multiple-scattering sequences in the medium and over the stationary distribution describing the motion of the scatterers. We use the ergodic assumption for a stationary medium, which assumes that all the multiple-scattering paths are time independent. Therefore, the ensembles of paths $\{C_n(T)\}$ and $\{C_n(0)\}$ are identical. The amplitude term in expression (52) thus becomes independent of T , i.e., independent of the motion of the scatterers. Its average over the configurations of disorder gives the diffuson, so that

$$\gamma_{12}(\mathbf{r}, T) \propto \sum_n P(\mathbf{r}_0, \mathbf{r}, n) \langle \exp\{i[\phi_n(T) - \phi_n(0)]\} \rangle, \quad (53)$$

where $P(\mathbf{r}_0, \mathbf{r}, n)$ is the contribution of the scattering paths of length n to the classical probability expression (6) for a source in \mathbf{r}_0 . It results from this expression that the insight relative to the motion of the scatterers appears only in the phase factors $\Delta\phi_n(T) = \phi_n(T) - \phi_n(0)$. The degree of coherence may be calculated along these lines either for the diffuson (d) or the cooperon (c), which differ only by the phase factors $\Delta\phi_n^{(c,d)}(T) = \phi_n(T) \pm \phi_n(0)$.

To proceed further, let us assume a Brownian motion of the scatterers characterized by a diffuson constant D_b [not to be mistaken for the diffuson coefficient $D = \frac{1}{3}vl_e$ obtained in the diffuson approximation of Eq. (7)]. Then, for long enough multiple-scattering trajectories parameterized by the time $t = n\tau_e$, we have⁵

$$\begin{aligned} \langle \exp[i\Delta\phi_n(T)] \rangle &\simeq \exp\left[-\frac{1}{2}\langle \Delta\phi_n^2(T) \rangle\right] \\ &= \exp[-n\tau_e/\tau_\phi(T)] = \exp[-t/\tau_\phi(T)], \end{aligned} \quad (54)$$

where we have introduced the phase-coherence time $\tau_\phi = (\tau_e/2k^2)(1/D_b T)$ beyond which the interference effects disappear. A phase-coherence length can be defined as well through the relation $L_\phi = (D\tau_\phi)^{1/2}$. We emphasize here again that decoherence gives rise to an irreversible loss of interference patterns. We may think of other controlled and reversible ways of changing the interference pattern, such as, for instance, an Aharonov–Bohm magnetic flux in weakly localized electronic systems³⁶ leading to the Sharvin–Sharvin effect.

Only trajectories with time $t = n\tau_e$ smaller than the phase coherence time $\tau_\phi(T)$ can interfere. This defines the mesoscopic regime. Unlike electronic systems, for which this term has been coined and where L_ϕ is very small (typically L_ϕ is a few micrometers at mK temperatures), the phase-coherence length in optical systems might be quite large so that coherence effects are observable up to macroscopic scales.

A quantity often measured in the multiple-scattering regime of photons is not the degree of coherence $\gamma_{12}(T)$ but instead the intensity-correlation function $g_2(T)$ defined by

$$g_2(T) = \frac{\langle I(T)I(0) \rangle}{\langle I(0) \rangle^2} - 1, \quad (55)$$

with the usual relation $I(T) = |E(T)|^2$ between the intensity and the field. Consequently, the degree of coherence of relation (53) is expressed in terms of the diffuson in the form

$$\gamma_{12}(\mathbf{r}, T) = \int_0^\infty dt P(\mathbf{r}, t) \exp(-tT/2\tau_b\tau_e), \quad (56)$$

where the time $\tau_b = 1/4D_b k^2$ accounts for the motion of one scatterer. If we remember that the time parameter $t = n\tau_e$ measures the length of the multiple-scattering trajectories, we interpret the previous relation by saying that the characteristic dephasing time for the two complex amplitudes paired in trajectories of length n is proportional to τ_b/n . Then, the longer the multiple-scattering trajectory, the shorter its coherence time. For $n = 1$, we recover the single-scattering case, namely, the time-correlation function decreases exponentially with the time τ_b . Multiple scattering offers this interesting advantage of probing the correlation function at times very short compared to τ_b , i.e., to single scattering. The typical length of the longest diffusive trajectories obtained experimentally corresponds to values of n between 10^2 and 10^3 . This sensitivity of the long multiple-scattering trajectories to dephasing is now used very frequently to characterize dense solutions of classical scatterers and to study their dynamics. It has been given the name diffusive-wave spectroscopy.^{11,37–39}

We have seen when studying the coherent backscattering peak that the long multiple-scattering trajectories corresponding to the cooperon contribute mainly at small angles. In the presence of dephasing, the trajectories longer than the phase-coherence length are washed out, leading to a rounding of the backscattering peak. Something similar happens to the degree of coherence $\gamma_{12}(T)$. We can make this statement more quantitative by noting that for a semi-infinite system, the expression of the degree of coherence $\gamma_{12}(T)$ can be deduced from expression (16) of the coherent albedo $\alpha_c(\theta)$, provided we make the formal replacement

$$Dk_\perp^2 \leftrightarrow \frac{1}{\tau_\phi} = \frac{T}{2\tau_e\tau_b}. \quad (57)$$

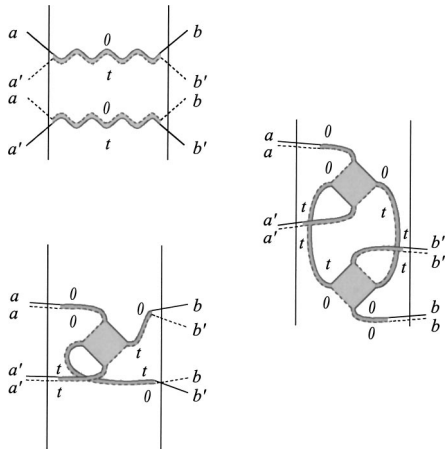


Fig. 11. Trajectories contributing to the time-correlation functions.

To proceed further and to calculate the intensity-correlation function $g_2(T)$, we note that it involves the average of the product of four electric fields. Hence, by using the pairing rules of the amplitudes as in the calculation of the angular-correlation function (see Fig. 11), we obtain¹¹

$$g_2(T) = |\gamma_{12}(T)|^2. \quad (58)$$

In the limit $T = 0$, we recover the second moment of the Rayleigh law, Eq. (23). For a slab with fixed ingoing and outgoing waves, we obtain, by using relations (56) and (58), the corresponding expression $g_2^{(1)}(T)$ ^{12,38}

$$g_2^{(1)}(T) = F_1(L/L_\phi) = \left(\frac{L/L_\phi}{\sinh L/L_\phi} \right)^2, \quad (59)$$

with $L_\phi(T) = l_e(2\tau_b/3T)^{1/2}$. It can also be derived from relation (30) by replacing $1/q_a$ by $L_\phi(T)$. The intensity-correlation function decreases exponentially with time T and with a characteristic time T^* given by $T^* \approx \tau_b(L/l_e)^2$.

An advantage of the measurement in transmission as compared with reflection is that only long multiple-scattering trajectories that transit the sample do enter. For such trajectories, the diffuson approximation is justified, while in reflection, for instance for the albedo, short trajectories also contribute which cannot be described using the diffuson approximation.

Relation (58) is correct whenever diffuson crossings can be neglected. Higher-order terms in powers of $1/g$ for the time-correlation function are obtained from the possible pairings of the four complex amplitudes as represented in Fig. 11. For the case of one crossing, we note that, unlike $g_2^{(1)}(T)$, the corresponding correlation-function $g_2^{(2)}(T)$ involves two kinds of diffusons: those whose amplitudes are taken at the same time and those taken at times 0 and T . The calculation can be achieved along the same lines as for the angular-correlation function $C_{aba'b'}^{(2)}$ with the result^{26,30}

$$g_2^{(2)}(T) = \frac{2}{g} F_2(L/L_\phi), \quad (60)$$

where the function $F_2(x)$ has been defined in Eq. (44). Unlike $g_2^{(1)}(T)$, this correlation function decreases at large times like a power law. It is smaller than $g_2^{(1)}(T)$ by a factor of $1/g$, so that its measurement requires one to get rid of $g_2^{(1)}(T)$. This can be achieved by an angular integration over the outgoing directions or, equivalently, by averaging over a large number of speckle spots.^{39,40}

The correlation-function $g_2^{(3)}(T)$ with two diffuson crossings is more involved. We can no longer derive it from the angular-correlation function and replace q_a by $1/L_\phi$ since, as noted before, $g_2^{(3)}$ has no angular structure. By using the rules we have set for phase boxes and expression (26) for P in the slab geometry, and by replacing k_\perp by $1/L_\phi$, we obtain⁵

$$g_2^{(3)}(T) = \int_0^L \int_0^L dz dz' P^2(1/L_\phi, z, z') = \frac{L^4}{8D^2} F_3(L/L_\phi), \quad (61)$$

so that

$$g_2^{(3)}(T) = \frac{1}{g^2} F_3(L/L_\phi), \quad (62)$$

where we have defined

$$F_3(x) = \frac{3}{2} \frac{2 + 2x^2 - 2 \cosh 2x + x \sinh 2x}{x^4 \sinh^2 x}. \quad (63)$$

We recover the result $C^{(3)}(0) = 2/15$ for $L_\phi \rightarrow \infty$. The expression of $g_2^{(3)}(T)$ given by Eq. (61) involves the integral of P^2 . This originates from the closed loop appearing in Fig. 11. This expression looks quite close to those proposed in Ref. 35, but it gives a much slower time dependence that should be sought in the behavior of the distribution of all closed loops inside the slab, and not only those reaching the boundaries. The term $g_2^{(3)}(T)$ is much more difficult to observe³⁵ since it is proportional to $1/g^2 \approx 10^{-4}$.

Unlike $g_2^{(1)}(T)$, the two other contributions to the time-correlation function of the intensity cannot be written in terms of the degree of coherence $\gamma_{12}(T)$. This is due to the presence of the phase boxes that entangle the complex amplitudes of the diffusons. This situation is, in a sense, analogous to those encountered for the time-correlation functions of photons for which there is no relation between the quantum degrees of first- and second-order coherence.⁴¹ Nevertheless, the single time that characterizes all the correlation functions is the phase-coherence time τ_ϕ . This is a consequence of our assumption of scalar waves. We expect different results when we take into account the polarization of the wave and its coupling to degrees of freedom of the scatterers as in cold atomic gases.^{13,14,42,43}

ACKNOWLEDGMENTS

This work is supported in part by a grant from the Israel Academy of Sciences, by the fund for promotion of Research at the Technion, and by the French-Israeli Arc-en-ciel program.

Corresponding author E. Y. Akkermans may be reached by e-mail to eric@physics.technion.ac.il.

REFERENCES AND NOTES

1. "Mesoscopic quantum physics," in *Proceedings of the Les Houches Summer School, Session LXI*, E. Akkermans, G. Montambaux, J. L. Pichard, and J. Zinn-Justin, eds. (North-Holland, Amsterdam, 1995).
2. Y. Imry, "The physics of mesoscopic systems," in *Directions in Condensed Matter Physics*, G. Grinstein and G. Mazenko, eds. (World Scientific, Singapore, 1986).
3. Y. Imry, *Introduction to Mesoscopic Physics (Mesoscopic Physics and Nanotechnology)* 2nd ed. (Oxford University, Oxford, UK, 2002).
4. S. Chakraverty and A. Schmid, "Weak-localization: the quasi-classical theory of electrons in a random potential," *Phys. Rep.* **140**, 193–236 (1986).
5. E. Akkermans and G. Montambaux, *Mesoscopic Physics of Electrons and Photons* (EDP Sciences-CNRS, Paris, 2004).
6. *Scattering and Localization of Classical Waves in Random Media*, P. Sheng, ed. (World Scientific, Singapore, 1990).
7. E. Akkermans and G. Montambaux, "Coherent multiple scattering in disordered media," <http://arxiv.org/abs/cond-mat/0104013>.
8. M. Born and E. Wolf, *Principles of Optics*, 7th ed. (Cambridge University, Cambridge, UK, 1999), Chap. X.
9. L. Mandel and E. Wolf, *Optical Coherence and Quantum Optics* (Cambridge University, Cambridge, UK, 1995).
10. B. J. Berne and R. Pecora, *Dynamic Light Scattering with Applications to Chemistry, Biology, and Physics* (Wiley, New York, 1976).
11. G. Maret and P. E. Wolf, "Multiple light scattering from disordered media: The effect of Brownian motion of scatterers," *Z. Phys. B: Condens. Matter* **65**, 409–414 (1987).
12. P. E. Wolf and G. Maret, "Dynamics of Brownian particles from strongly multiple light scattering," in *Scattering in Volumes and Surfaces*, M. Nieto-Vesperinas and J. C. Dainty, eds. (North-Holland, Amsterdam, 1990).
13. G. Labeyrie, F. de Tomasi, J.-C. Bernard, C. A. Müller, C. Miniatura, and R. Kaiser, "Coherent backscattering of light by cold atoms," *Phys. Rev. Lett.* **83**, 5266–5269 (1999).
14. T. Jonckheere, C. A. Müller, R. Kaiser, C. Miniatura, and D. Delande, "Multiple scattering of light by atoms in the weak localization regime," *Phys. Rev. Lett.* **85**, 4269–4272 (2000).
15. A. A. Golubentsev, "Suppression of interference effects in multiple scattering of light," *Sov. Phys. JETP* **59**, 26–39 (1984).
16. E. Akkermans and R. Maynard, "Weak localization of waves," *J. Phys. (France) Lett.* **46**, L1045–1053 (1985).
17. E. Akkermans, P. E. Wolf, and R. Maynard, "Coherent backscattering of light by disordered media: Analysis of the peak line shape," *Phys. Rev. Lett.* **56**, 1471–1474 (1986).
18. E. Akkermans, P. E. Wolf, R. Maynard, and G. Maret, "Theoretical study of the coherent backscattering of light by disordered media," *J. Phys. (Paris)* **49**, 77–98 (1988).
19. B. G. Hoover, L. Deslauriers, S. M. Grannell, R. E. Ahmed, D. S. Dilworth, B. D. Athey, and E. N. Leith, "Correlations among angular wave component amplitudes in elastic, multiple-scattering random media," *Phys. Rev. E* **65**, 026614–026621 (2002).
20. P. E. Wolf and G. Maret, "Weak localization and coherent backscattering of photons in disordered media," *Phys. Rev. Lett.* **55**, 2696–2699 (1985).
21. M. P. van Albada and A. Lagendijk, "Observation of weak localization of light in a random medium," *Phys. Rev. Lett.* **55**, 2692–2695 (1985).
22. D. S. Wiersma, M. P. van Albada, B. A. van Tiggelen, and A. Lagendijk, "Experimental evidence for recurrent multiple-scattering events of light in disordered media," *Phys. Rev. Lett.* **74**, 4193–4196 (1995).
23. A precursor of this effect has been observed in L. Tsang and A. Ishimaru, "Backscattering enhancement of random discrete scatterers," *J. Opt. Soc. Am. A* **1**, 836–839 (1984).
24. J. W. Goodman, *Statistical Optics* (Wiley, New York, 1985).
25. B. Shapiro, "Large-intensity fluctuations for wave propagation in random media," *Phys. Rev. Lett.* **57**, 2168–2171 (1986).
26. R. Berkovits and S. Feng, "Correlations in coherent multiple scattering," *Phys. Rep.* **238**, 135–172 (1994).
27. I. Freund, M. Rosenbluh, and S. Feng, "Memory effects in propagation of optical waves through disordered media," *Phys. Rev. Lett.* **61**, 2328–2331 (1988).
28. S. Hikami, "Anderson localization in a nonlinear- σ -model representation," *Phys. Rev. B* **24**, 2671–2679 (1981).
29. M. C. W. van Rossum and T. M. Nieuwenhuizen, "Multiple scattering of classical waves: microscopy, mesoscopy and diffusion," *Rev. Mod. Phys.* **71**, 313–371 (1999).
30. S. Feng and P. A. Lee, "Mesoscopic conductors and correlations in laser speckle patterns," *Science* **251**, 633–639 (1991).
31. S. Feng, C. Kane, P. A. Lee, and A. D. Stone, "Correlations and fluctuations of coherent wave transmission through disordered media," *Phys. Rev. Lett.* **61**, 834–837 (1988).
32. R. Pnini and B. Shapiro, "Fluctuations in transmission of waves through disordered slabs," *Phys. Rev. B* **39**, 6986–6994 (1989).
33. S. Washburn, "Fluctuations in the extrinsic conductivity of disordered metals," *IBM J. Res. Dev.* **32**, 335–346 (1988).
34. B. L. Al'tshuler and B. Shklovskii, "Repulsion of energy lev-

- els and conductivity of small metal samples,” *Sov. Phys. JETP* **64**, 127–141 (1986).
35. F. Scheffold and G. Maret, “Universal conductance of light,” *Phys. Rev. Lett.* **81**, 5800–5803 (1998).
 36. A. G. Aronov and Y. V. Sharvin, “Magnetic flux effects in disordered conductors,” *Rev. Mod. Phys.* **59**, 755–779 (1987).
 37. D. J. Pine, D. A. Weitz, P. M. Chaikin, and E. Herbolzheimer, “Diffusing wave spectroscopy,” *Phys. Rev. Lett.* **60**, 1134–1137 (1988).
 38. M. J. Stephen, “Temporal fluctuations in wave propagation in random media,” *Phys. Rev. B* **37**, 1–5 (1988).
 39. G. Maret, “Dynamic speckle correlations,” in *NATO Advanced Study Institute on Waves and Imaging through Random Media*, P. Sebbah, ed. (Kluwer Academic, Dordrecht, The Netherlands, 2001), pp. 413–434.
 40. F. Scheffold, W. Hartl, G. Maret, and E. Matijevic, “Observation of long-range correlations in temporal-intensity fluctuations of light,” *Phys. Rev. B* **56**, 10942–10952 (1997).
 41. R. Loudon, *The Quantum Theory of Light* (Clarendon, Oxford, UK, 1986).
 42. E. Akkermans, C. Miniatura, and C. A. Müller, “Phase coherence times in the multiple scattering of photons by cold atoms,” <http://arxiv.org/abs/cond-mat/0206298>.
 43. C. A. Müller and C. Miniatura, “Multiple scattering of light by atoms with internal degeneracy,” *J. Phys. A* **35**, 10163–10188 (2002).

Conduction quantique et Physique mésoscopique

μΕΣΟΣ

PHY 560B

Gilles Montambaux

users.lps.u-psud.fr/montambaux

06 janvier 2017

Mécanique quantique → Théorie des bandes
 * Métaux
 * Isolants
 * Semiconducteurs

Comprendre les propriétés macroscopiques, à partir du microscopique :

Description microscopique, physique quantique
 + physique statistique

Ex: Recouvrement des orbitales atomiques
 + électrons dans potentiel périodique
 → Théorie des bandes
 + interactions e-e
 → Supraconductivité, magnétisme

2

Propriétés macroscopiques

Transport électronique :

description « classique » : Drude,
 principe de Pauli : Sommerfeld, ...
 Conductivité et loi d'Ohm

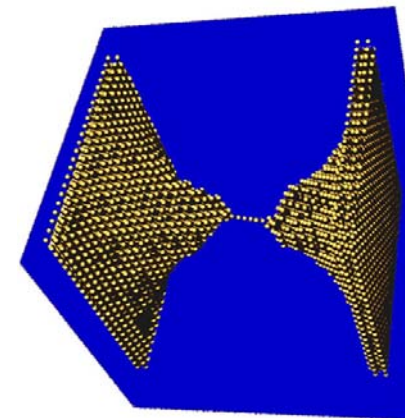
$$G = \sigma \frac{S}{L}$$

Au-delà : interférences quantiques :

Exemple :

La résistance R (ou la conductance G) ne dépend pas uniquement du matériau, mais aussi de la façon dont on le contacte au monde macroscopique

3



$$G \neq \sigma \frac{S}{L}$$

La conductance de ce contact d'atomes d'Or est-elle reliée à la conductivité de l'Or, suit-elle la loi d'Ohm?

NON → nouveaux concepts, nouveaux outils

4

PHY 560B
 Conduction quantique et physique mésoscopique
 cours 2016-2017
 Gilles Montambaux Département de Physique

quelques transparents... ouverts en images... du cours

EOLY (long à télécharger 35 Mo)

5 janvier	Cours	Introduction, les matériaux	PC1 aspects : densité d'états, conductivité
12 janvier	Cours	De transport classique au transport quantique	PC2 structure de Landau, états de bord PC3 transparence
19 janvier	Cours	Conductance d'un circuit quantique	PC3 conductance = multiterminaux =
9 février	Cours	Conductance d'un circuit quantique (aH)	PC4 conductance = multiterminaux = (aH)
10 février	Cours	Effet Hall quantique	PC5 effet Hall quantique dans le graphène PC6 transparence
		DM	
24 février	Cours	Désordre et cohérence de phase	PC6 Transport cohérent 1D, Equation de diffusion
3 mars	Cours	Localisation faible	PC7 Anisotropie négative, oscillations Shubnikov-Shernov
10 mars	Cours	Fluctuations universelles de conductance	PC8 Anisotropie cohérente PC9 transparence Simulation 1D site de rétrodiffusion cohérente
13 mars	Cours	Propriétés spectrales des systèmes complexes Un éditeur vers la théorie des matrices aléatoires Mélange de Wigner P(0) pour des matrices 2*2	PC9

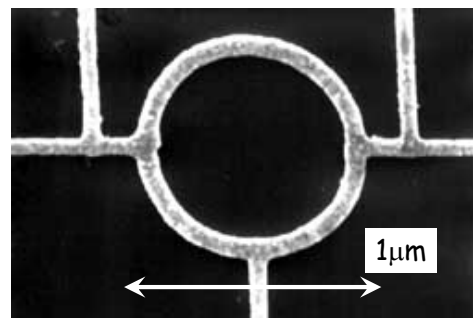
Pour en savoir plus :
 Lecture : A.H. Feynman
 There is plenty of room at the bottom
 In 1959, A.H. Feynman gave a conference on the developments possible in the microtechnology - on the occasion
 Un article de vulgarisation sur l'effet Aharonov-Bohm
 Les interférences quantiques et l'effet Aharonov-Bohm

Un petit panorama de la recherche en Physique Mésoscopique, articles récents, sites et autres adresses

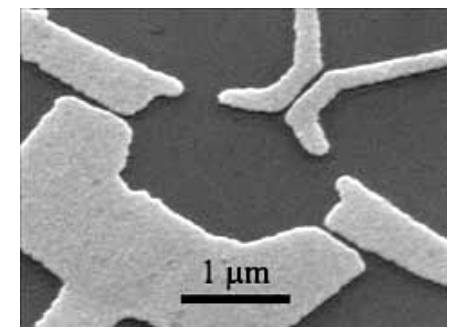
Quelques références : Sites

Quelques sites à parcourir
 Master 2 : Concepts fondamentaux de la Physique
 Le Laboratoire de Mécanique et Nanotechnique - LMPN - MRS
 Laboratoire de Mécanique et Nanotechnique - LMPN - MRS
 Le Laboratoire National de Métrologie et d'Essais - LNE - Trappes
 http://www.lne.fr/

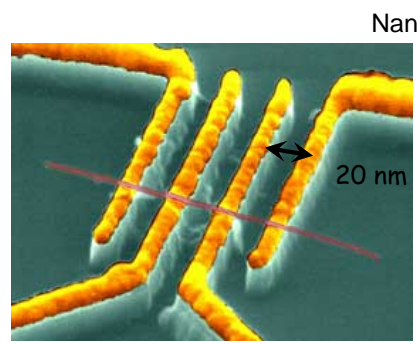
<https://users.lps.u-psud.fr/Montambaux/X-meso.htm>



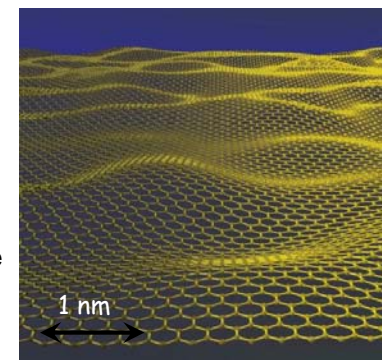
anneau métallique Cu



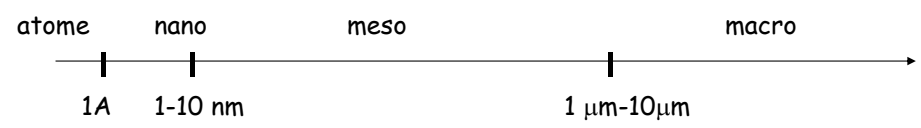
Gaz 2D, semiconducteur (AlGaAs)



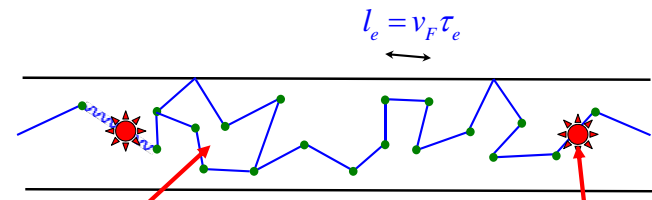
Nanotube de carbone



Graphène



l_e libre parcours moyen : distance entre collisions élastiques



interférence

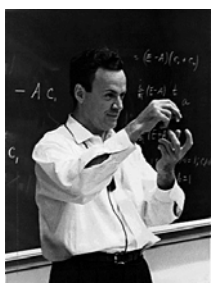
Les collisions élastiques ne brisent pas la cohérence de phase

Les interactions avec un degré de liberté extérieur (phonons, électrons, impuretés de spin) brisent la cohérence de phase

$L_\phi(T)$

longueur de cohérence de phase

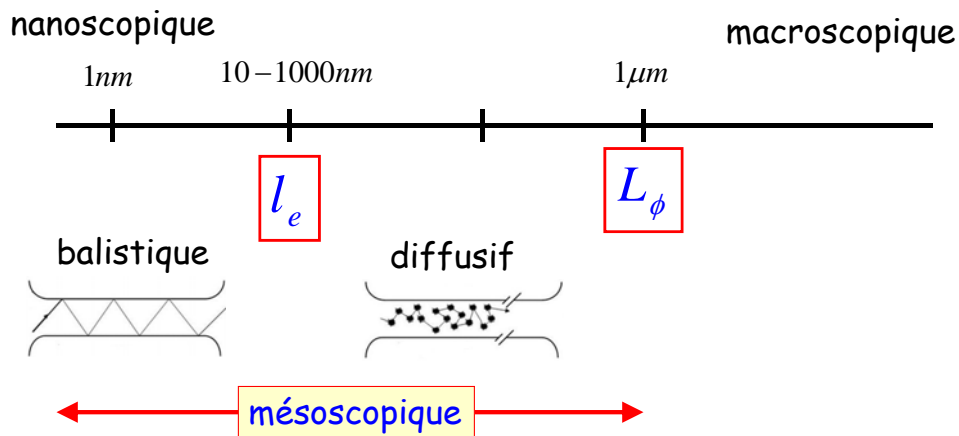
$$L_\phi = \sqrt{D\tau_\phi}$$



There's Plenty of Room at the Bottom
An Invitation to Enter a New Field of Physics
 1959

R.P. Feynman (1918-1988)

A partir de quelle échelle, de nouveaux concepts sont-ils indispensables?



l_e Libre parcours moyen : distance entre collisions élastiques

$L_\phi(T)$ Longueur de cohérence de phase

La loi d'Ohm



1789-1854

$$I = GV$$

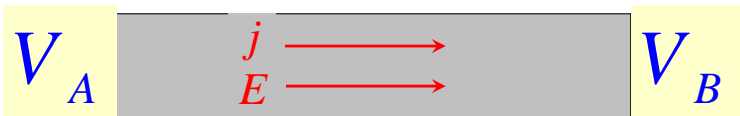
$$G = \sigma \frac{S}{L}$$

G conductance, σ conductivité



10

La loi d'Ohm



$$\vec{j} = \sigma \vec{E}$$

$$I = GV$$

$$I = jS = \sigma E S$$

$$G = \sigma \frac{S}{L}$$

$$V = V_A - V_B = E L$$

G conductance, σ conductivité

11

$$G = \sigma \frac{S}{L}$$

Loi d'Ohm

$$\sigma = \frac{ne^2\tau_e}{m}$$

Formule de Drude-Sommerfeld

Validité ?

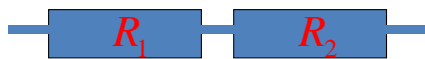
Pas d'inférences quantiques
Régime diffusif

$$L > L_\phi$$

$$L > l_e$$

Nouveaux comportements non classiques

$$R \neq R_1 + R_2$$



$$R \neq \frac{\rho L}{S}$$

$$G \neq G_1 + G_2$$

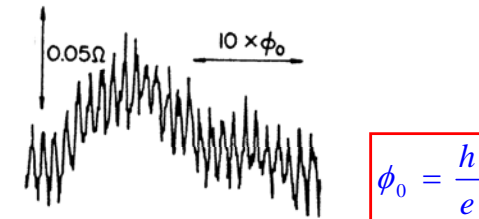
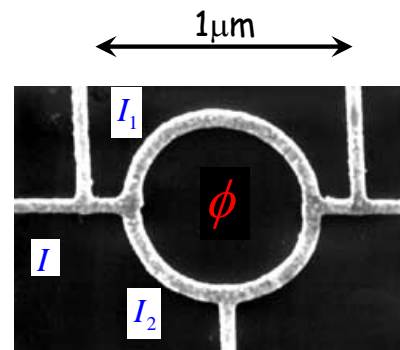


$$G \neq \frac{S}{\rho L}$$

13

R. Webb (IBM, 1985)

expérience fondatrice de la physique mésoscopique



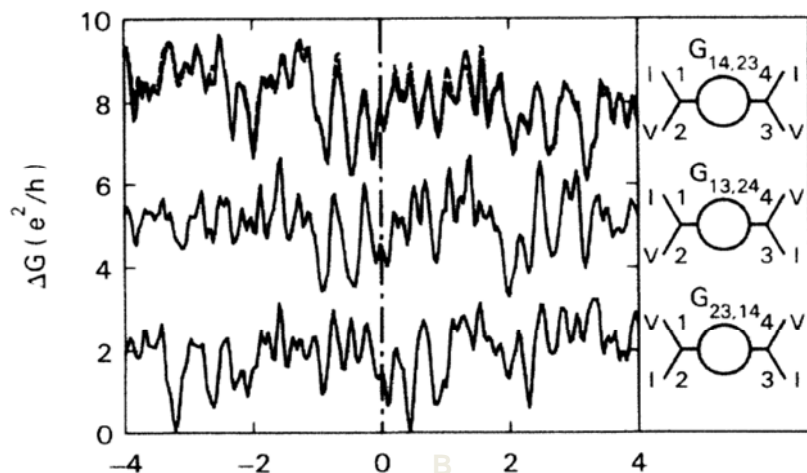
$$I = I_1 + I_2 + I_{\text{int}} \cos \frac{2\pi\phi}{\phi_0}$$

Interférences entre ondes électroniques (cf. trous d'Young)

Effet Aharonov-Bohm (1959)

$$L < L_\phi$$

14

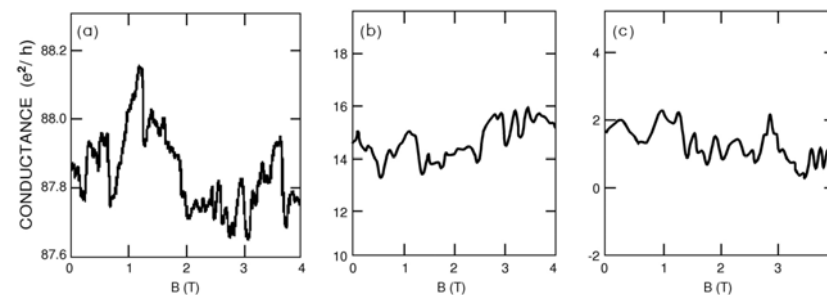


On mesure une conductance et pas une conductivité

La conductance dépend de la façon dont on la mesure

15

Fluctuations universelles de conductance

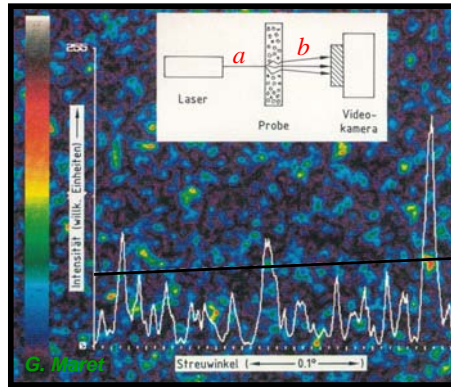


« Figure d'interférence » complexe qui dépend de la configuration précise du désordre dans l'échantillon

$$\delta G = \sqrt{G^2 - \bar{G}^2} \sim \frac{e^2}{h}$$

Cf. Speckle en optique

16



Speckle - Tavelure en optique

Analogies électronique - optique
conductance - coefficient de transmission

Au lieu de $\sigma = \frac{ne^2\tau}{m}$

Une nouvelle description du transport électronique :

La formule de Landauer

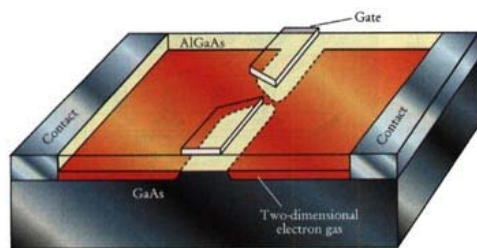
$$G = 2 \frac{e^2}{h} T$$

La conductance est un coefficient de transmission

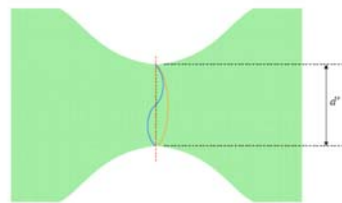
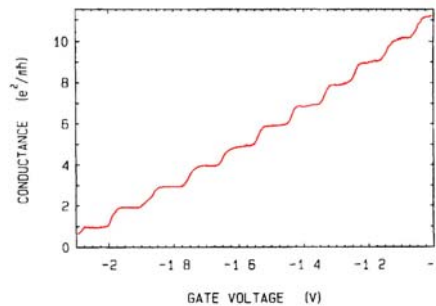
Analogies avec l'optique, les guides d'onde

Quantification de la conductance (1988)

Un point contact quantique



$$G = 2 \frac{e^2}{h} M = 2 \frac{e^2}{h} \text{int} \left[\frac{2W}{\lambda_F} \right]$$



ANALOGUE À UN GUIDE D'ONDE

$\frac{e^2}{h}$ Quantum de conductance

Plan du cours

Les matériaux

Les limitations de la description classique
Le domaine de la physique mésoscopique

Formalisme de Landauer : conductance d'un circuit quantique
Transport balistique

L'effet Hall quantique

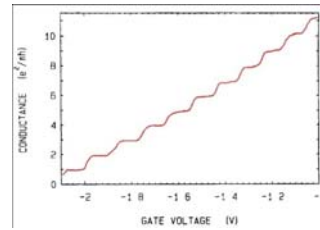
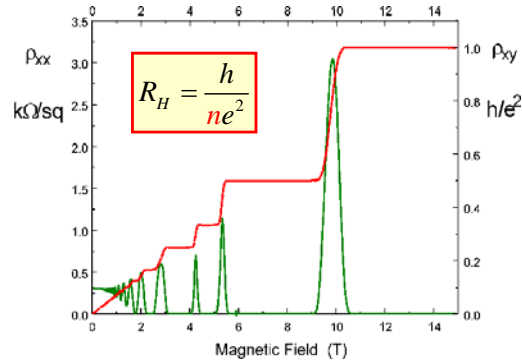
Cohérence de phase et désordre

De l'équation de Schrödinger à l'équation de diffusion
Localisation faible et rétrodiffusion cohérente en optique
Fluctuations universelles de conductance et speckle en optique

La théorie des matrices aléatoires

La physique du graphène

L'effet Hall quantique (1981)

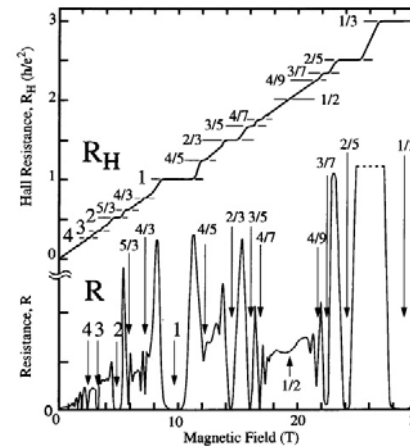


cf. quantification de la conductance, mais ici très grande précision

→ Etalon de résistance

$$R_K = \frac{h}{e^2} = 25812,807449(86) \Omega$$

L'effet Hall quantique fractionnaire (1983)

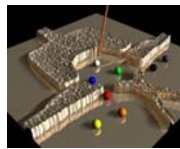
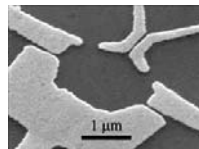
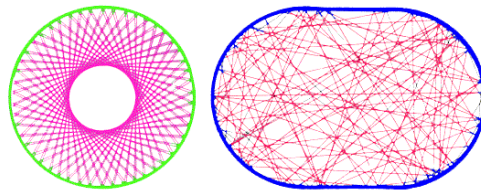
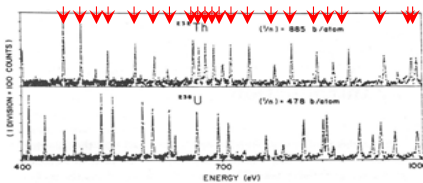


$$R_H = \frac{q}{p} \frac{h}{e^2}$$

Mise en évidence de charges fractionnaires !

Théorie des matrices aléatoires

Décrire les niveaux d'énergie d'un système complexe



Noyaux

Billards quantiques

Autres systèmes quantiques

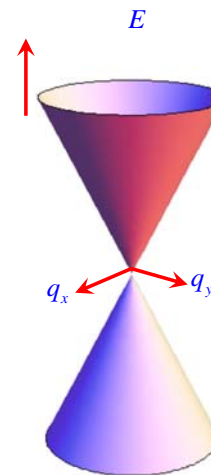
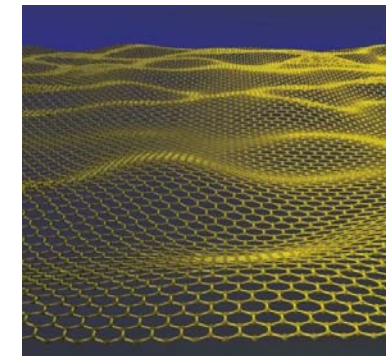
atome d'hydrogène sous champ magnétique

systèmes désordonnés (métaux)

Modes acoustiques, mécaniques, électromagnétiques

Zéros de la fonction ζ de Riemann

La physique du graphène



Système parfaitement 2D
Particules de masse nulle !
Applications importantes



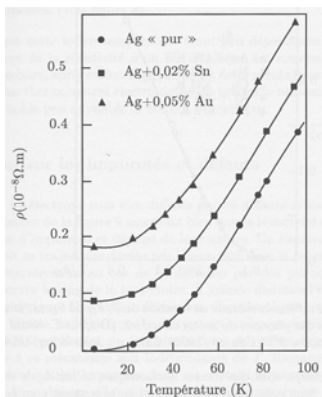
Equation de Dirac

Particule massive

Retour sur la conductivité de Drude - Sommerfeld

$$\sigma(T) = \frac{ne^2\tau(T)}{m}$$

Loi de Matthiessen



$$\frac{1}{\tau(T)} = \frac{1}{\tau_e} + \frac{1}{\tau_{in}(T)}$$

Collisions élastiques

Collisions inélastiques :
électron-phonon

conductivité résiduelle :

$$\sigma = \frac{ne^2\tau_e}{m}$$

$$\sigma = e^2 D \rho_0$$

Formule de Drude

Relation d'Einstein

τ_e

Temps de collision, temps de vie élastique

$$l_e = v_F \tau_e$$

Libre parcours moyen

Validité limitée à des échantillons macroscopiques

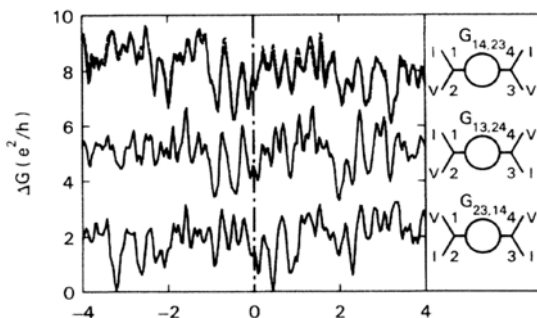
$$l_e \ll L$$

« régime diffusif »

26

Fluctuations reproductibles de conductance

$$l_e \ll L < L_\phi$$

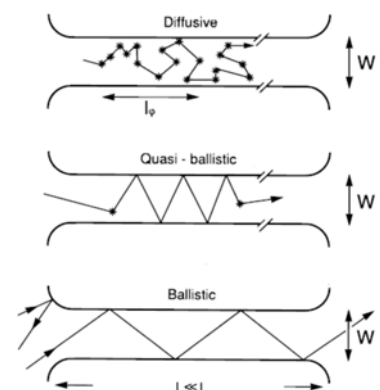


La description de Drude-Einstein est une description moyenne, correcte si

Comment aller au-delà de la moyenne, et décrire ces fluctuations ?

→ **Domaine de la Physique Mésoscopique**

27



nanoscopique

mésoscopique

macroscopique

1nm

10-1000nm

1μm

ballistique

l_e

diffusif

L_ϕ

28

Les matériaux

Les techniques de fabrication

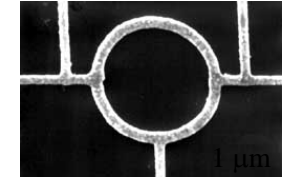
Les matériaux

Métaux

Or, Argent, Cuivre,...

$$l_e \sim 10 \text{ nm}$$

Transport diffusif

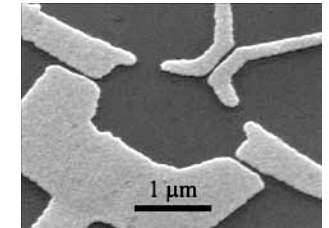


Hétérostructures de semiconducteurs

GaAs-AlGaAs

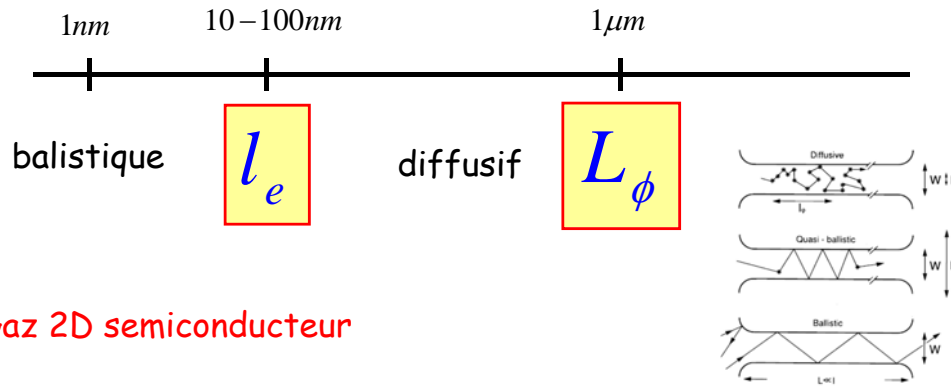
Transport diffusif ou balistique

$$l_e \sim 10 \mu\text{m}$$



Gaz 2D

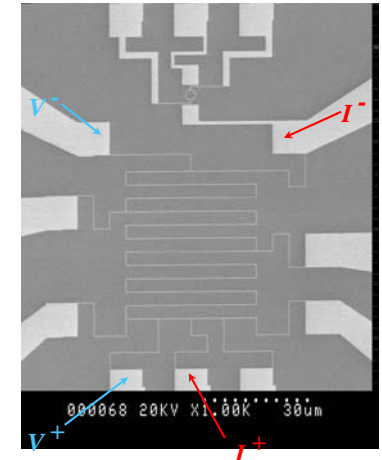
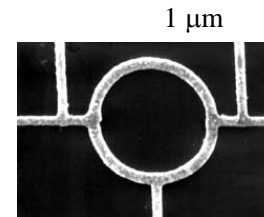
Métal

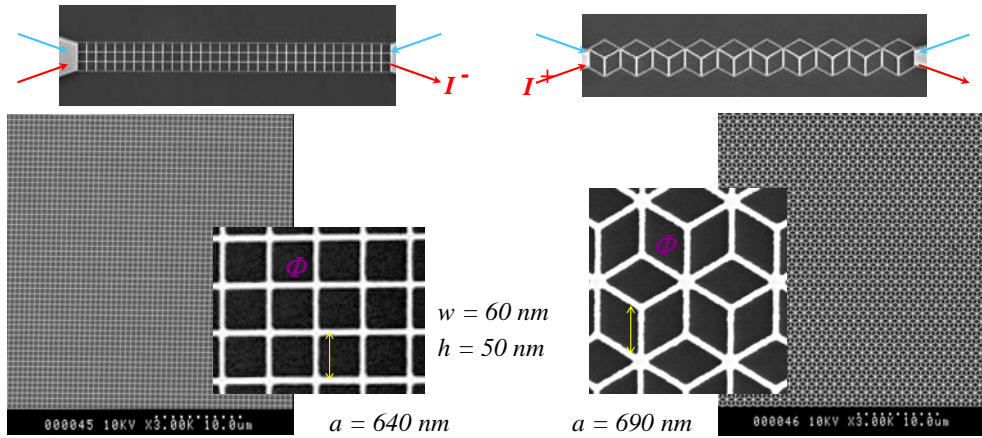


Gaz 2D semiconducteur



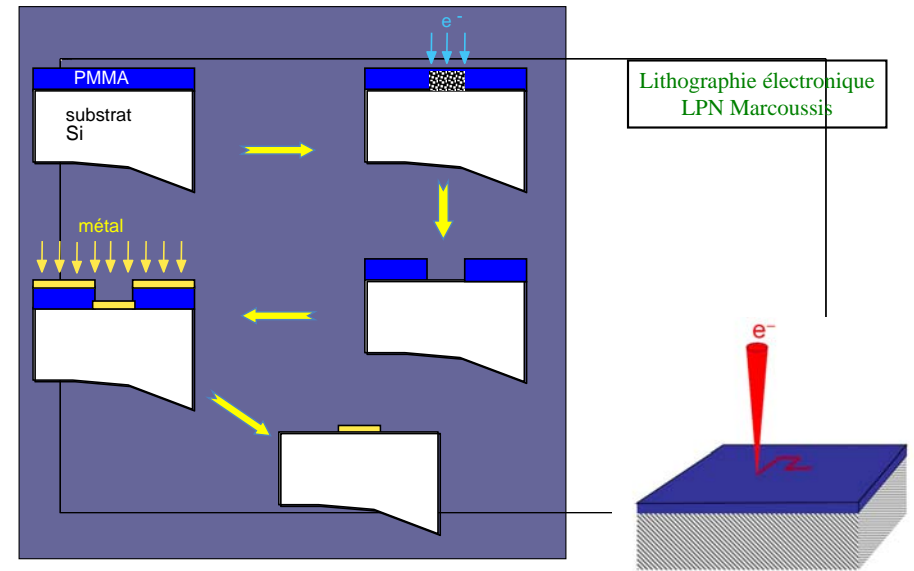
Fil métallique gravé : exemples





Institut Néel, Grenoble

Nanofabrication



Ag 6N (99.999%)
SPEC-CEA Saclay

Leica EBPG5000+



Lithographie électronique
LPN Marcoussis

LABORATOIRE DE PHOTONIQUE ET DE NANOSTRUCTURES

Marcoussis

CENTRE NATIONAL DE LA RECHERCHE SCIENTIFIQUE - UPR20

Présentation du laboratoire

PRÉSENTATION

EMPLOIS



RECHERCHE

SÉMINAIRES



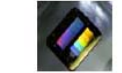
TECHNOLOGIE



COLLABORATIONS



FAITS MARQUANTS



RECHERCHER
SUR LE SITE



■ Présentation

Le Laboratoire de Photonique et de Nanostructures -LPN- (51 chercheurs, 41 ingénieurs et techniciens, et une soixantaine de doctorants et post-doctorants) est une unité propre du Centre National de Recherche Scientifique -CNRS- rattachée à deux instituts, l'Institut de Physique -INP- et l'Institut des Sciences de l'Ingénierie et des Systèmes -INSIS-.

Le LPN est l'une des 6 centrales du premier cercle du réseau RENATECH.

Sa vocation première est l'avancement coordonné de la recherche fondamentale et de la recherche appliquée, tant pour les recherches internes au laboratoire que pour celles développées en partenariat avec d'autres laboratoires publics ou privés, en s'appuyant sur l'exploitation et le développement de ses compétences technologiques.

Voici un lien vers l'[organigramme du LPN](#).

Les **8 groupes de recherche** du laboratoire développent leurs activités autour de quatre thèmes de recherche principaux :

[Photonique](#) [Nano-Electronique](#) [Matériaux](#) [Microfluidique et Nano-Biotechnologie](#)

et 2 thèmes de recherche transverses :

[Composants et systèmes opto-électroniques](#)

[Nano-Technologie](#)

www.lpn.cnrs.fr

c2n.cnrs.fr/



Le projet

Le Centre de Nanosciences et de Nanotechnologies (C2N) s'installera en 2017 à Paris-Saclay dans le quartier de l'École polytechnique. Il sera un futur pôle de référence nationale en matière ...

En savoir plus »



Le C2N en chiffres

Première centrale de technologie académique d'Ile de France 410 personnes dont 120 chercheurs et enseignant-chercheurs, 95 ingénieurs, techniciens et administratifs, 125 doctorants et post-doctorants 18 ...

En savoir plus »



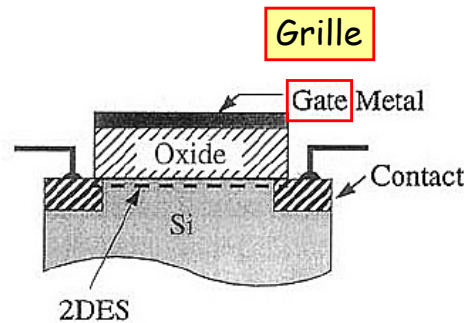
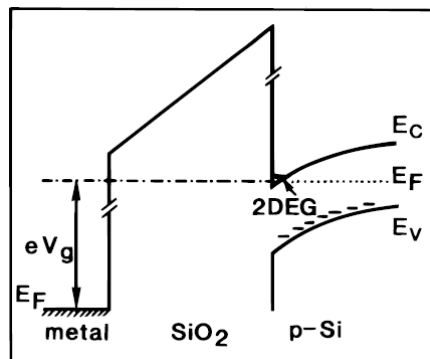
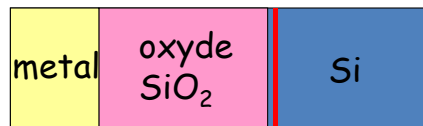
Les grandes étapes

Décembre 2011 : Décision de financement dans le cadre des investissements d'avenir avec le CNRS comme Maître d'ouvrage Mars 2013 : Sélection de la maîtrise d'œuvre. Mandataire ...

En savoir plus »

Si-MOSFET

1959 Bell labs

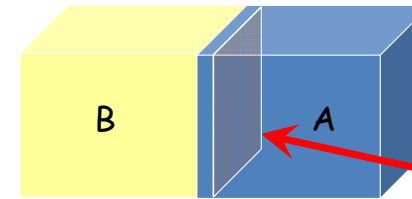


Metal-Oxide-Semiconductor Field Effect Transistor

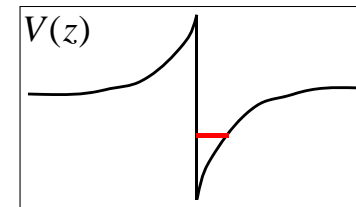
Hétérostructures de semiconducteurs

Gaz 2D, très grande mobilité

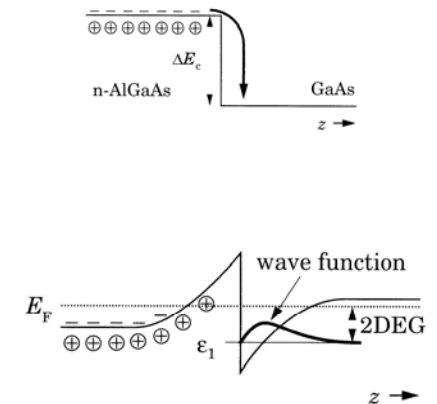
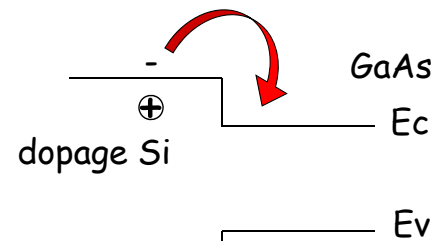
Principe : un puits de potentiel confine les électrons à l'interface de deux semiconducteurs différents.



2DEG : gaz d'électrons bidimensionnel



Hétérostructures de semiconducteurs III-V



Dopage modulé : les porteurs libres sont éloignés des donneurs

PERIODIC TABLE OF THE ELEMENTS

http://www.kf-split.hr/periodni/en/

Copyright © 1998-2003 EnG (en@kf-split.hr)

For more information and downloads please visit ---> <http://www.periodni.com/en/download.html>

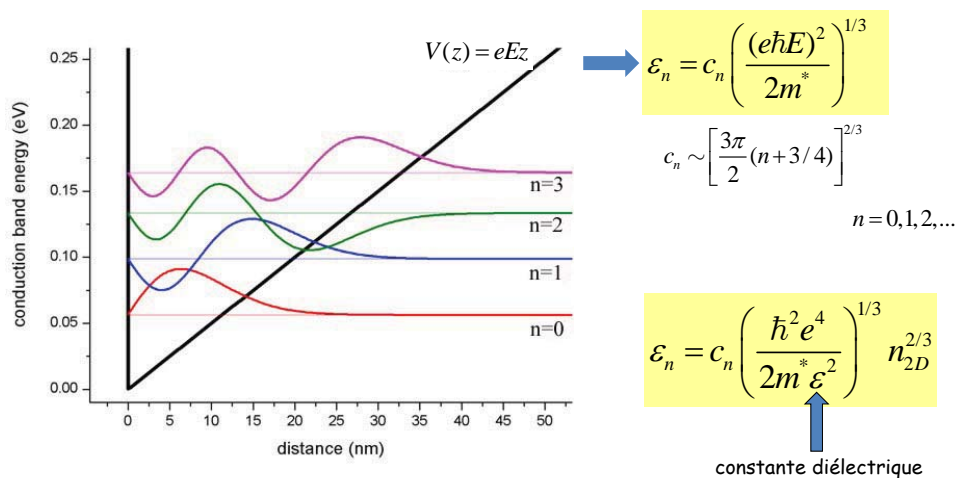
Dopage n de AlGaAs par Si

13	IIIA	14	IVA	15	VA
5	10.811	6	12.011	7	14.007
B		C		N	
BORON		CARBON		NITROGEN	
13	26.982	14	28.086	15	30.974
Al		Si		P	
ALUMINIUM		SILICON		PHOSPHORUS	
31	69.723	32	72.64	33	74.922
Ga		Ge		As	
GALLIUM		GERMANIUM		ARSENIC	

III

V

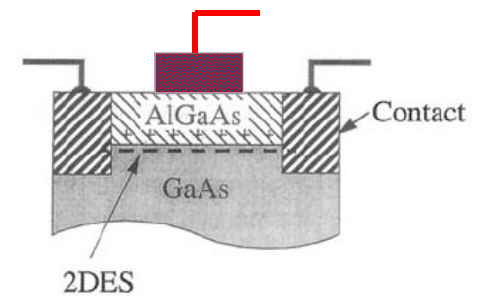
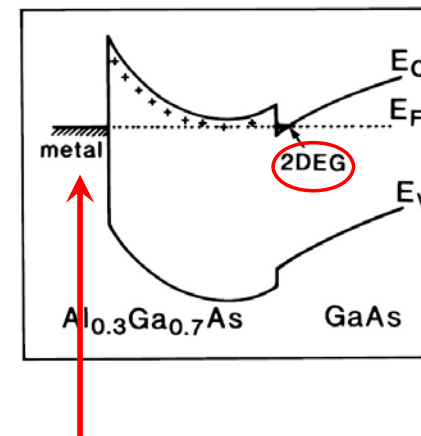
Gaz d'électrons dans un potentiel 1D triangulaire



Les niveaux sont quantifiés dans la direction z
mouvement libre dans le plan xy, avec une masse effective

$$\epsilon(k) = \frac{\hbar^2}{2m^*} (k_x^2 + k_y^2) + \epsilon_n$$

$$m^* \sim 0,067 m_e$$



HEMT
MODFET

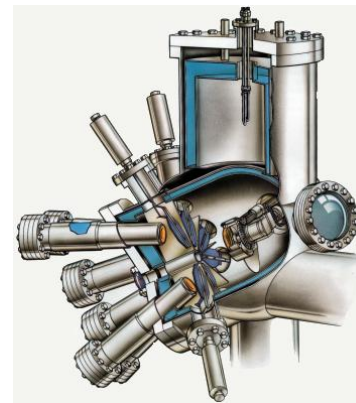
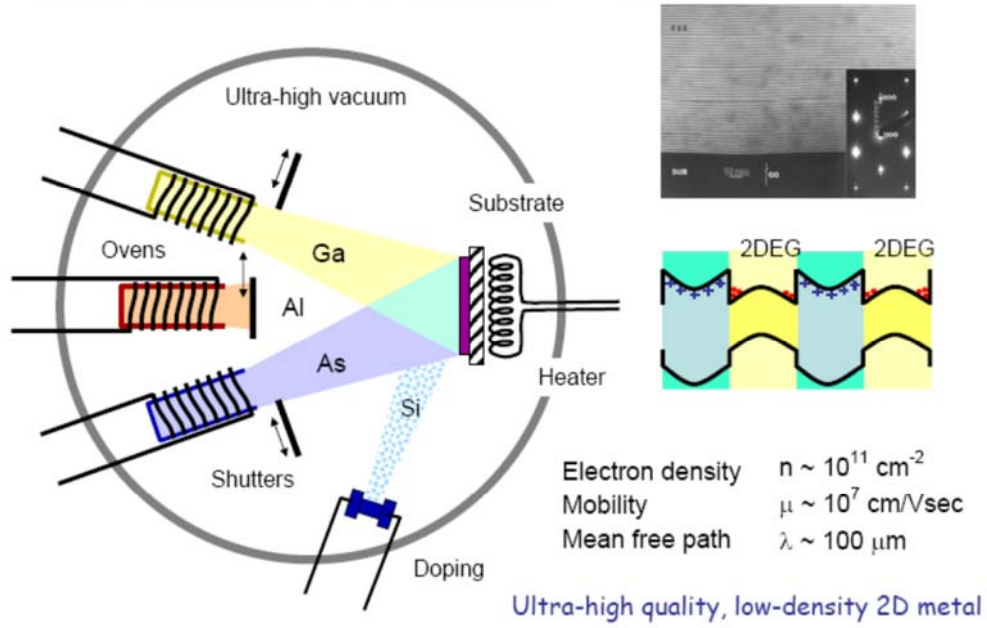
Une grille métallique module la densité électronique

$$n_{2D} = \frac{C(v_G - v_T)}{e}$$

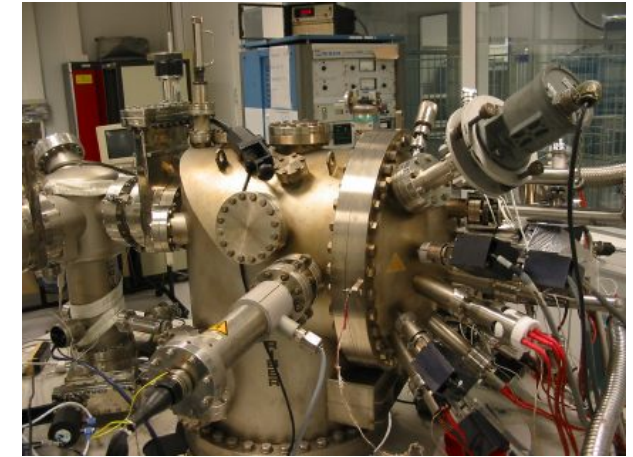
Les charges libres sont éloignées des impuretés donneuses → bonne mobilité

Bell labs, 1968

Molecular Beam Epitaxy (MBE)



MBE



LPN, Marcoussis